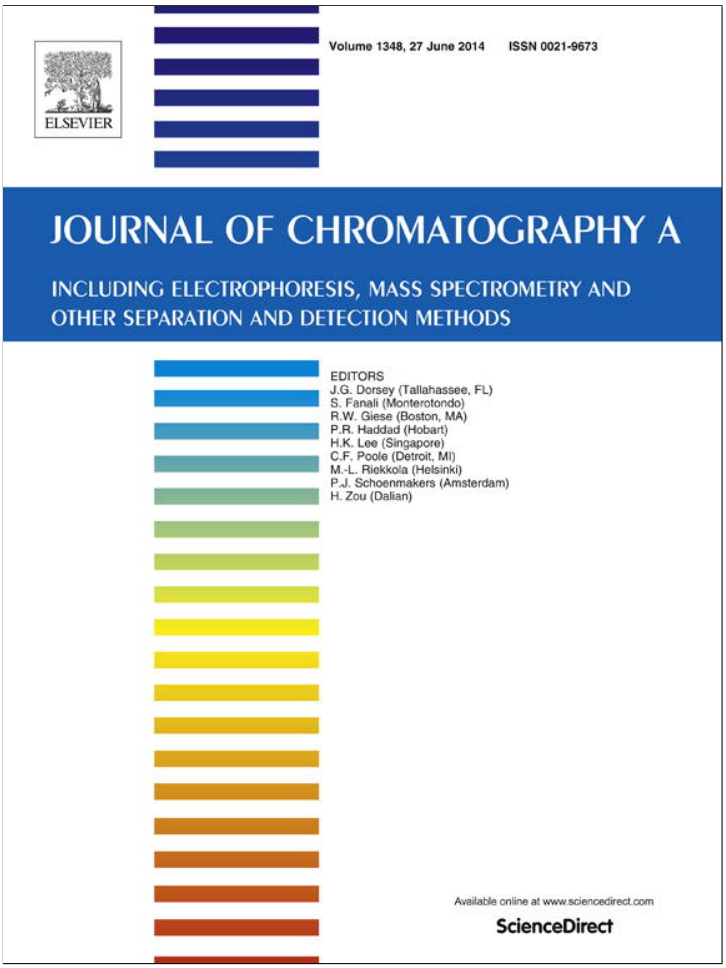

Journal of Chromatography A, 1348 (2014) 1–16

Contents lists available at ScienceDirect

Journal of Chromatography A

journal homepage: www.elsevier.com/locate/chroma

Review

Metal-organic frameworks in chromatography

Kareem Yusuf*, Ahmad Aqel, Zeid ALOthman

Advanced Materials Research Chair, Department of Chemistry, College of Science, King Saud University, P.O. Box 2455, Riyadh 11451, Saudi Arabia

ARTICLE INFO

Article history:
Received 17 February 2014
Received in revised form 14 April 2014
Accepted 28 April 2014
Available online 4 May 2014

Keywords:
Metal-organic frameworks
High-performance liquid chromatography
Gas chromatography
Capillary electrochromatography

ABSTRACT

Metal-organic frameworks (MOFs) emerged approximately two decades ago and are the youngest class of porous materials. Despite their short existence, MOFs are finding applications in a variety of fields because of their outstanding chemical and physical properties. This review article focuses on the applications of MOFs in chromatography, including high-performance liquid chromatography (HPLC), gas chromatography (GC), and other chromatographic techniques. The use of MOFs in chromatography has already had a significant impact; however, the utilisation of MOFs in chromatography is still less common than other applications, and the number of MOF materials explored in chromatography applications is limited.

Contents

1. Introduction

Metal-organic frameworks (MOFs) are crystalline, highly ordered framework systems synthesised via the self-assembling combination of organic ligands and inorganic metals or metal-oxo units (secondary building units, SBUs) using strong bonds to form a permanent, porous open crystalline framework [1,2]. The inorganic part of MOFs could be selected with various dimensionalities, creating chains (1D), layers (2D) and frameworks (3D) [3].

The term coordination polymers (coordination networks) was previously used to describe MOFs [4–8] due to their similarity with coordination chemistry, especially the polyhedral inorganic parts [3]. The differences in vocabulary are usually due to the researchers who created the structures, although they are almost using the same types of materials [9]. However, Tranchemontagne et al. identified distinct differences between coordination polymers and MOFs [10]. Since the term "MOF" was introduced in 1995 by Yaghi and co-workers [11], there has been intensive research that led to approximately 20,000 different MOFs over the past two decades [1].

In comparison to conventional porous inorganic frameworks, such as zeolites or carbon-based materials, the active surface areas of MOFs are considerably large, reaching 7140 $m^2 g^{-1}$ [12]. Inorganic frameworks also have limited diversity because they accept only a few cations [13–19], mostly limited to Al, Si and chalcogens [20], whereas MOFs exist with almost all possible cations up to tetravalent atoms [3]. The variety of elements used in MOFs, along with the large choice of organic linkers, provides a substantial number of possibilities for creating new MOFs.

* Corresponding author. Tel.: +966 596245977.
E-mail addresses: dr_kareemyusuf@yahoo.com, kmahmoud@ksu.edu.sa (K. Yusuf).

http://dx.doi.org/10.1016/j.chroma.2014.04.095
0021-9673/

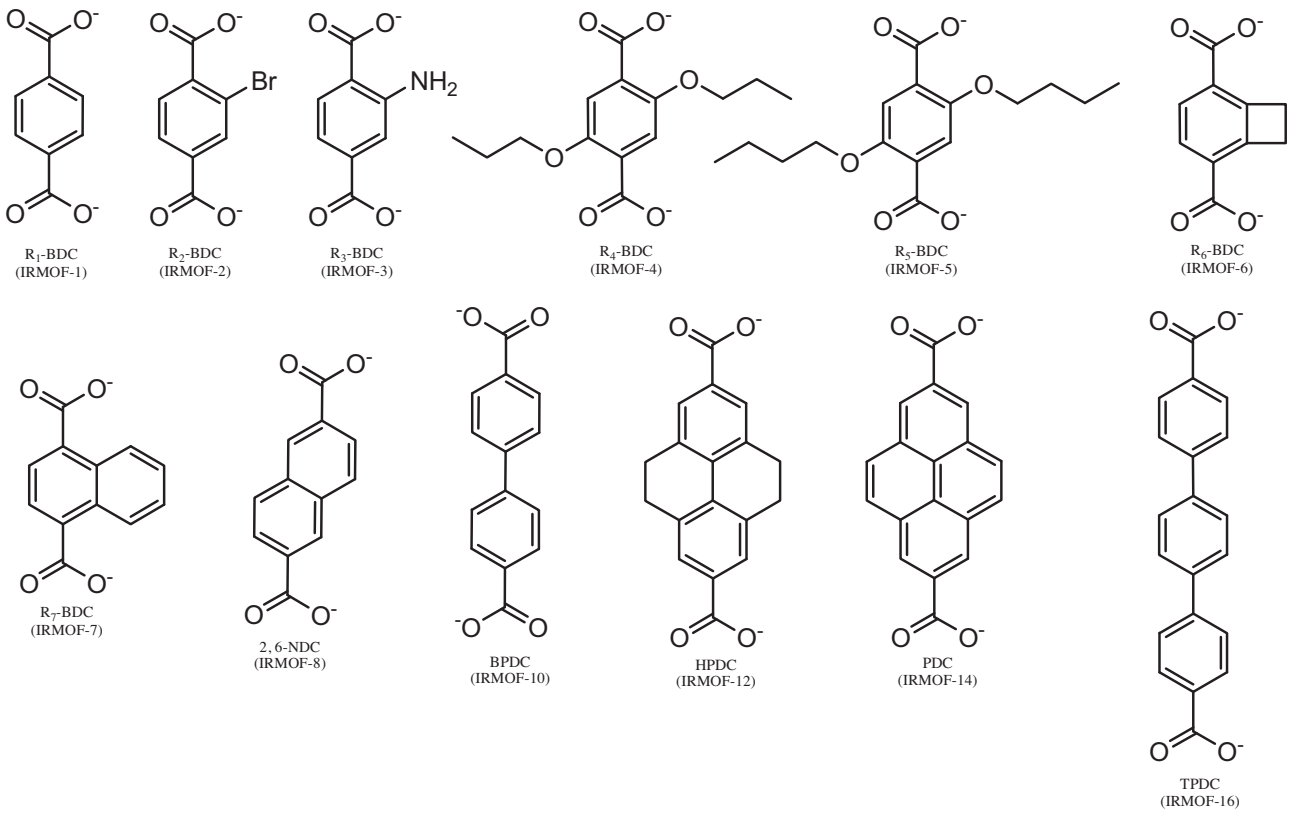

Fig. 1. Organic linkers of IRMOF-*n* (*n* = 1 through 7, 8, 10, 12, 14, and 16) labelled appropriately.

Conversely, inorganic frameworks often utilise a variety of templates or structure-directing compounds. These templates are removed via oxidation, and as a consequence, the removal of the template can result in the collapse of the framework. In MOFs, the framework template is directed by the SBU and the organic ligands [21,22].

MOFs hold the world records for the most porous materials with the largest pore aperture (98 Å) [23], the highest specific surface area (10,400 $m^2\,g^{-1}$) [12] and the lowest density (0.13 $g\,cm^{-3}$) [24]. MOF structures have synthetic flexibility to change their size and nature without changing their topology, which is called the isoreticular principle (from the Greek term *iso* meaning same and the Latin term *reticulum* meaning net). The isoreticular character allows MOFs to hold macromolecules, such as vitamins and proteins, and to increase the interaction space within the pores. The ability of adding functional groups into the framework also give MOFs another advantage over other porous materials by allowing post-synthetic modification [1]. The designable structures of MOFs, along with their unique physical, thermal and chemical properties, have led to their utilisation in numerous applications, including chromatographic applications.

2. Structural overview

Metal-organic frameworks consist of two main components: a metal-containing component (cationic part) and an organic component (anionic part) that combine through strong bonding to produce a well-defined highly ordered framework [25]. One of the main properties of MOFs is self-assembly, which affords the desired structure framework. Self-assembly is defined by George Whitesides as "a process where pre-designed components assemble in a determined structure without the intervention of human operators" [26]. The important characteristics of the metal-containing part are their coordination numbers and geometries, which play an important role in directing the MOF structures. The other important property is the organic linkers, which have a great influence over the shape of the constructed MOF. The organic linkers (or ligands) generally contain coordinating functional groups, such as carboxylates, phosphates, sulphonates, amines, or nitriles, which serve an essential function in locking the metal ions strongly into their positions. Fig. 1 shows some examples of such organic linkers in MOFs [27].

It is difficult, but not impossible, to obtain such MOF structures from simple metal ions and organic linkers because the ions provide little directionality [27]. This limited directionality results in mobility around the metal ion and more than one possible structure, which yields generally inconsistent results, as exemplified by the frameworks based on Cu ions and bipyridine and related linkers [28–35].

To design a network molecular structure such as a MOF, we can start with well-defined and rigid molecular building blocks (MBBs) that will maintain their structure during the construction process [36,37]. Alternatively, the use of well-defined reaction conditions to form these building blocks in situ is an equally applicable method to design this type of extended structure, which is called reticular synthesis [37]. Yaghi et al. described reticular synthesis as "the process of carefully designing a rigid molecular building blocks into stable highly ordered networks, which are held together by strong bonding" [27]. Reticular chemistry [38] – sometimes referred to as 'crystal engineering' – is concerned with the design and synthesis of compounds formed from finite SBUs joined by strong chemical bonds [27]. SBU is an abbreviation that refers to the geometry of the building units defined by the points of extension and describes either the organic or inorganic part of the MOF structure [27]. In reticular synthesis, the metal-containing (cationic) SBUs cannot be isolated, so they have to be constructed in situ with careful control over the reaction conditions, including the mixing stoichiometry, reaction temperature and time, solvent system, ionic strength and

concentration, addition of weak acids or bases and the nature of the counter ions [27]. Conversely, organic (anionic) SBUs are pre-synthesised using conventional organic synthetic methods [39]. A basic prediction supported by experimental results [40] is that when symmetrical SBUs are attached to simple linkers, only one high symmetry structure will be formed [41,42]. In other words, by using such a strategy to synthesise MOF structures, it is possible to control and predict the structure of the resulting framework as well as its properties for a specific application [27].

Crystal structures have been described in terms of nets since the beginning of crystallography. In these nets, atoms are the vertices and the bonds are the links (edges) between them. These nets are a special type of periodic graph [43]. In structures such as those of zeolites [44], tetrahedrally coordinated atoms (Si, Al, P, etc.) are joined by —O— links to form a four-coordinated net of tetrahedral vertices with the —O— links acting as the edges [10]. In the case of MOFs, polyatomic groups act as the vertices and edges of the net [45].

In 2000, O'Keeffe et al. [41] defined some topological rules for controlling the structures of porous solids, including MOFs. Starting with some MOF structures that correspond to extended versions of simple structures (diamond, sodalites, etc.), they developed a system of symbols for naming, classifying and identifying these topological structures based on the invariance of the topology of structures for any chemical associations, and this system is now in wide use. In this work, O'Keeffe and his group outlined the rules for the Reticular Chemistry Structure Resource (RCSR), which collected approximately 1600 structures in a database searchable by symbol, name or keywords [45]. In the RCSR, the net topologies of the MOFs are described using a three-letter symbol in bold lowercase; the symbol is either a three-letter symbol (such as ***pqr***) or a three-letter symbol with an extension as in ***pqr-a***, which is called the *augmented* net in which a cluster of vertices replaces the vertex of the original net [46].

The first major breakthrough towards the design of rigid frameworks based on the previous description of SBUs was revealed in MOF-2 [47] and MOF-5 [48]. In MOF-5, there are $Zn_4O(CO_2)_6$ units containing four ZnO_4 tetrahedra with a common vertex and six carboxylate C atoms that define an octahedral SBU, each linked by six chelating 1,4-benzenedicarboxylate (BDC) units, to give a cubic framework. In MOF-5 (a cubic network), the vertices are the octahedral SBUs, and the edges are the benzene molecules. The resulting structure was found to have an exceptional porosity of 61% (indicated by its gas sorption measurements), stability (indicated by thermal analysis and single crystal X-ray diffraction studies) and a high surface area of 2320 $m^2\,g^{-1}$ (indicated by Brunauer–Emmett–Teller, BET, measurements) [48]. These values are much higher than the conventional counterparts, such as zeolites and activated carbon [49]. The polyatomic cationic rigid clusters that form the vertices of MOF-5 could explain its exceptional stability [27].

Changing the chemical composition, functionality, and molecular size of crystalline materials in a systematic way that maintains the topology was a challenge for material scientists [38,50]. In 2002, Eddaoudi et al. [51] presented the first isoreticular [IR] structures based on the cubic ***pcu*** skeleton of MOF-5 (IRMOF-1) up to IRMOF-16 with a 16-member family. The isoreticular structures of MOFs differ in the nature of the functional groups within the organic linker and/or in the length of its edges by using an expanded version of the organic linker without changing the original network topology.

In IRMOF-2 through IRMOF-7, BDC links with R groups representing bromo, amino, *n*-propoxy, *n*-pentoxy, cyclobutyl, or fused benzene functional groups (Fig. 1) result in structures with almost the same size but different functionalities within the voids, whereas in IRMOF-8 (2,6 NDC linker; 2,6-naphthalenedicarboxylate) through IRMOF-16, pore expansion occurs due to the use of progressively longer organic linkers. However, the large space in the expanded forms tends to form interpenetrating structures, which indicates that two or more frameworks grow and interfere with each other. Fig. 1 shows the absence of IRMOF-9, IRMOF-11, IRMOF-13, and IRMOF-15 due to interpenetration. These MOFs used BPDC (biphenyl-4,4′-dicarboxylate), HPDC (4,5,9,10-tetrahydro-2,7-pyrenedicarboxylate), PDC (2,7-pyrenedicarboxylate), and TPDC (*p*-terphenyl-4,4″-dicarboxylic acid) as linkers, respectively. The degree of interpenetration could be controlled by changing the reactant concentrations and reaction conditions. Non-interpenetrating counterparts have been successfully achieved for all linkers in the previous work by using diluted reaction conditions.

Another effective way to prevent interpenetration is to select a suitable topology for MOFs that inhibits interpenetration [52]. MOF-177 [$Zn_4O(BTB)_2$] (BTB; 4,4′,4″-benzene-1,3,5-triyl-tribenzoate) is a good example of interpenetration inhibition by using a triangular organic linker, giving rise to the ***qom*** net structure. Even in the case of the expanded isoreticular structures of MOF-177, which yields MOF-180 [$Zn_4O(BTE)_2$] (BTE; 4,4′,4″-(benzene-1,3,5-triyl-tris(ethyne-2,1-diyl))tribenzoate) and MOF-200 [$Zn_4O(BBC)_2$] (BBC; 4,4′,4″-(benzene-1,3,5-triyl-tris(benzene-4,1-diyl))tribenzoate) [53], the networks remain non-interpenetrating despite the high porosity of these MOFs (89% and 90% for MOF-180 and MOF-200, respectively).

Another interesting MOF is known as HKUST-1 [$Cu_3(BTC)_2$] (BTC; 1,3,5-benzene tricarboxylate) [54]; it is composed of Cu paddlewheel [$Cu_2(CO_2)_4$] SBUs and a tritopic organic linker, BTC. Many isoreticular structures have been produced using several tritopic linkers to give the same ***tbo*** net structure of HKUST-1 [24,55–58]. MOF-399 [$Cu_3(BBC)_2$] is the largest member of this family. Its cell volume is 17.4 times that of HKUST-1. MOF-399 has the highest void fraction (94%) and the lowest density (0.126 $g\,cm^{-3}$) of any reported MOF [24]. Isoreticular structures can also be synthesised using different metal ions to afford the same network structure. The HKUST-1 isoreticular series was prepared by replacing the Cu metal ion with another metal, such as Zn(II) [59], Fe(II) [60], Mo(II) [61], Cr(II) [62], or Ru(II) [63].

The superior adsorption ability of MOFs has been observed in gas storage and gas separation applications. The primary adsorption sites for Ar and N_2 within the internal surface of the large-pore open MOF-5 have been identified using single-crystal X-ray diffraction [64]. The study revealed a total of eight adsorption sites. The adsorption sites included the zinc oxide units $Zn_4O(CO_2)_6$, the faces, and the organic linker edges. Furthermore, it has been revealed that using tritopic organic linkers based on alkyne rather than phenylene groups will increase the adsorption sites and consequently increase the surface area [65]. Using such organic linkers led to NU-110 [Cu_3(BHEHPI); BHEHPI = 5,5′,5″-((((benzene-1,3,5-triyltris(benzene-4,1-diyl))tris(ethyne-2,1-diyl))-tris(benzene-4,1-diyl))tris(ethyne-2,1-diyl))triisophthalate], which has the largest surface area of a porous material to date with a surface area of 7140 $m^2\,g^{-1}$ [1].

Using the BET method to calculate the surface area per unit weight of microporous materials, such as MOFs, is widely accepted [66]. However, a major problem accompanied with using this method is that separating the processes of mono-multilayer adsorption from micropore filling is difficult [67]. Therefore, the surface areas of MOFs obtained using the BET method are thought to not reflect the true internal surface area but rather should be considered a type of "apparent" or "equivalent BET area" [68,69]. Recently, a simulation study was performed to test the applicability of the BET method for determining the surface areas of MOFs [70,71]. The BET surface areas from the simulated isotherms agreed with the experimental surface areas reported in the literature. For

many practical applications, such as gas storage and gas separation, calculating the surface area per volume is more useful [1]. When we used this fact, we found that MOF-5 with a surface area of 2200 m^2 cm^{-3} is the best MOF material for such purposes, compared with NU-110, which has a surface area of 1600 m^2 cm^{-3}.

3. Applications in chromatography

The unique properties and the wide structural choices make MOFs attractive candidates for chromatographic applications (Table 1). Over the last few years, a substantial number of studies have demonstrated the potential of MOFs as a new class of chromatographic materials in the areas of gas and liquid chromatography. Yet only two specific review articles on the application of MOFs in separation science have been published [72,73]. MOFs have been either directly used without further modifications or engineered to meet the chromatographic challenges. They have been used as column packings, coatings or as a monolithic material in conventional or capillary columns. This work focuses on the use of MOF materials in chromatographic applications.

3.1. Gas chromatography applications

Gas chromatography (GC) is the most promising among the chromatographic techniques for employing MOFs as the stationary phase. Various MOF materials and column structures have been demonstrated in several publications for high resolution gas chromatography. In the following section, we will discuss the most significant and recent applications of MOFs in GC.

3.1.1. Packed columns

In 2006, Chen et al. introduced the first application of MOFs as a packing material in GC [74]. They used MOF-508 [Zn(BDC)(4,4′-Bipy)$_{0.5}$(DMF)(H_2O)$_{0.5}$] with a thermal stability of up to 360 °C as stationary phase for packed-column GC. A 120-cm chromatographic column, packed with single crystals of MOF-508 with sizes of 25–100 μm (3 g), was used in the study. The GC separation of natural gas was performed at an inlet pressure of 60 psi with helium as the carrier gas over a temperature range of 40–150 °C (Fig. 2). The unique features of MOF-508 are its 1D pores of 4.0 Å × 4.0 Å, which separate linear alkanes from branched alkanes.

The separation of isomers was investigated for the first time using a column packed with a MOF material by Finsy et al. [75]. They studied the separation of the C8 alkyl aromatic components *p*-xylene, *m*-xylene, *o*-xylene, and ethylbenzene (EB) on the metal-organic framework MIL-47 [$V^{IV}O$(BDC)] using vapour-phase adsorption and separation. The four isomers were found to have comparable Henry constants and adsorption enthalpies at temperatures between 230 and 290 °C. The adsorption capacity of the adsorption isotherms were strongly temperature dependent at 70, 110, and 150 °C. The adsorption selectivity generally increases as the partial pressure or degree of pore filling increases. The separation at a high degree of pore filling in the vapour phase is the result of differences in the packing modes of the C8 alkylaromatic components in the pores of MIL-47.

Gu et al. examined the adsorption and separation of xylene isomers and EB on two Zn-terephthalate MOFs (MOF-5 and MOF-monoclinic; [Zn_4O(BDC)$_3$]) using pulse gas chromatography, static vapour-phase adsorption, and breakthrough adsorption [76]. The two studied Zn-terephthalate MOFs, which showed different selectivities and efficiencies for the separation of xylene isomers and EB. Pulse GC experiments showed efficiency separation on MOF-5 (267 plate/m) than MOF-monoclinic (76 plates/m). On MOF-5, EB eluted first, while the other isomers eluted at the same time. The monoclinic MOF showed a preferable adsorption of *p*-xylene over the other isomers. The selectivity resulted mainly from the different sizes of pore windows in the Zn-terephthalate MOFs. The terephthalate linkers in MOF-5 form pores with a cross section approximate 12 Å in size. Therefore, the four isomers gave similar diffusion coefficients on MOF-5 without any size hindrance with respect to the kinetic diameters of xylene isomers and EB (5.85–6.85 Å). In MOF-monoclinic the extended "stack" SBU forming triangle pores with an edge length of ~7 Å. The small kinetic diameter of *p*-xylene (5.85 Å) resulting in the biggest diffusion coefficient on MOF-monoclinic and a preferable adsorption. The adsorption and separation of xylene isomers and EB were equilibrium controlled on MOF-5 and diffusion dominated on the monoclinic MOF. On the basis of the measured McReynolds constants [77], MOF-5 was characterised as a nonpolar stationary phase, whereas the monoclinic MOF was characterised as an intermediate polarity phase for gas chromatography.

Another study by Scott et al. showed that MOF-199 or HKUST-1 [Cu_3(BTC)$_2$)] packed columns provided selective retention of small Lewis-base organic analytes (Fig. 3) [78]. MOF-199 was chosen as the MOF material for this study because it was relatively easy to prepare, displayed an intermediate Lewis acidity and the pore size was appropriate for many small organic analytes. The study examined MOF-199 when loaded in stainless steel columns prepared from tubing cut to dimensions of 1.83–2.74 m × 3.18 mm od (2.1 mm id) at various concentrations (5.0%, 0.75% and 0.10%, w/w) on an inert support material (Chromosorb W HP) that had been deactivated with a low loading of a non-polar stationary phase (3% SE-30). The results showed that the MOF-199-containing stationary phase had limited thermal stability (220 °C) and a strong general retention for analytes. The Kováts index calculations showed selective retention relative to n-alkanes for many small Lewis-base analytes on a column that contained 0.75% Cu-BTC compared with an SE-30 control.

Borjigin et al. presented a 2D microporous MOF JUC-110 [Cd(H-thipc)$_2$·6H_2O] (thipc; (S)-4,5,6,7-tetrahydro-1H-imidazo[4,5-c]pyridine-6-carboxylate), with 1D hydrophilic channels of approximately 4.5 Å × 4.5 Å for GC separation [79]. The packed-column (180 mm long × 2 mm i.d.) was filled with samples of JUC-110 and utilised for the separation of alcohol-water mixtures. The GC separation showed that the ethanol and methanol can be separated from water with retention times of 0.36 min, 15.89 min and 8.84 min respectively. JUC-110 square channels excluded alcohols larger than and equals to 4.5 Å but accommodated smaller molecules including water and methanol. Because the size of methanol molecules fits better with the channels of JUC-110 than water molecules, water moves faster than methanol.

JUC-110 exhibits exceptional hydrothermal stability; even under treatment with boiling water for ten days, it retains its crystalline structure, which is rare among porous MOFs, especially 2D ones [79]. The low hydro-stability of MOFs is a feature that not fully understood until now. In the case of hydrophilic MOFs, the water binds to unsaturated metal sites, leading to structural changes and framework's collapse. While in hydrophobic MOFs, the metal containing SBU clusters act as "weak hydrophilic defects". A water cluster could fully displace one arm of a linker and which means the loss of the material's ordered structure [80]. However, JUC-110 showed poor thermal stability (≈200 °C).

The UiO-66 structure was developed by Cavka et al. [81]. The structure of this MOF is composed of a zirconium inorganic brick [Zr_6O_4 $(OH)_4(CO_2)_{12}$] linked with twelve terephthalate ligands (BDC). Bozbiyik et al. demonstrated the inverse shape-selective behaviour of UiO-66 in the adsorption and separation of linear and cyclic alkanes through a packed column [84]. Stainless steel chromatographic columns (300 mm long × 3.12 mm i.d.) filled with 500 mg pellets (UiO-66) with sizes of 530–600 μm were used. They found that cyclohexane fits better in the pores of UiO-66, leading to a more negative adsorption enthalpy and a decreased loss

Table 1
The most significant applications of metal-organic frameworks in chromatography.

MOF material	Surface area ($g\,cm^{-3}$)	Pore opening (Å)	Pore diameter (Å)	Thermal stability (°C)	Samples	Form	Ref.	Year
Gas chromatography								
MOF-508, Zn (BDC)(4,4′-Bipy)$_{0.5}$	946	4		360	Alkanes	Packed column	[74]	2006
					Xylene isomers & EB	Packed column	[76]	2010
					VOCs[b]	Packed column	[83]	2010
MOF-5, IRMOF-1 ($Zn_4O(BDC)_3$)	630–3046	7.5, 11.2	11, 15	400–480	Natural gases	Coated capillary	[95]	2011
					n-Alkanes	Coated capillary	[89]	2011
					POPs[a]	Coated capillary	[135]	2011
					VOCs	Packed column	[84]	2013
IRMOF-3, ($Zn_4O(NH_2$-$BDC)_3$)	1957	9.6		320	POPs	Coated capillary	[135]	2011
IRMOF-8, ($Zn_4O(2,6$-$NDC)_3$)	1362	12.5	41.8	300	VOCs	Packed column	[84]	2013
IRMOF-10, ($Zn_4O(BPDC)_3$)	265	16.7	132.6	300	VOCs	Packed column	[84]	2013
HKUST-1, MOF-199, ($Cu_3(BTC)_2$)	404–629	8, 9	12	220–280	Small Lewis-base analytes	Packed column	[78]	2011
					Small hydrocarbons	Coated capillary	[97]	2012
MIL-47(V), ($V^{IV}O(BDC)$)	800	8.5	8.5	350	Xylene isomers & EB	Packed column	[75]	2008
MIL-100(Fe), ([$(Fe_3OF_3(BDC)_3)$]. nH_2O)	2040	5.5–8.6	25–29	280	Alkane isomers	Coated capillary	[91]	2012
MIL-100(Cr), ([$(Cr_3OF_3(BDC)_3)$]·nH_2O)	2153	5.5–8.6	25–29	280	Alkane isomers	Coated capillary	[91]	2012
					Xylene isomers & EB	Coated capillary	[85]	2010
MIL-101(Cr), ($Cr_3O(H_2O)_2F(BDC)_3$)	2736–2907	12, 16	29, 34	300–330	n-Alkanes	Coated capillary	[89]	2011
					n-Alkanes	Coated capillary	[87]	2010
ZIF-7, (Zn(benzimidazolate)$_2$)		2.9	4.3	480	n-Alkanes	Coated capillary	[89]	2011
					Organic vapours and gases	Packed column	[136]	2010
ZIF-8, Zn(2-methylimidazole)$_2$	1504	3.4	11.4	380–550	Branched & linear alkanes	Coated capillary	[87]	2010
					n-Alkanes	Coated capillary	[89]	2011
JUC-110, ([Cd(H-thipc)$_2$]·$6H_2O$)		4.5		≈200	Alcohols from water	Packed column	[79]	2012
UiO-66, [$Zr_6O_4(OH)_4(BDC)_6$]		5–7	8–11	480–540	Alkanes & alkylbenzenes	Coated capillary	[88]	2012
	614.3		7.5–11		n-Hexane & cyclohexane	Packed column	[82]	2013
MOF-CJ3 [$HZn_3(OH)(BTC)_2(2H_2O)$ (DMF)]·H_2O	525	11.6	11.6	250	Alkanes & aromatic positional isomers	Coated capillary	[103]	2013
DMOF-1, [$Cu_2(BDC)_2$(DABCO)]	1026–1300				Light hydrocarbons	Coated capillary	[99]	2013
High performance liquid chromatography								
		8.5	8.5	330–385				
MIL-47(V), ($V^{IV}O(BDC)$)	750	Pore volume of 0.32 $cm^3\,g^{-1}$			Xylene isomers & EB	Packed column	[104]	2007
MIL-101(Cr), ($Cr_3O(H_2O)_2F(BDC)_3$)	2736–2907	12, 16	29, 34	300–330	Substituted aromatics	Packed column	[137]	2011
					Fullerenes	Packed column	[118]	2011
					Alkylaromatics	Packed column	[113]	2008
		8.5	8.5		Positional isomers	Packed column	[116]	2012
MIL-53(Al), ($Al^{III}(OH)(BDC)$)	940–1038			330–385	Wide range of analytes	Packed column	[117]	2012
		Pore volume of 0.50 $cm^3\,g^{-1}$						
MIL-100(Fe), ([$(Fe_3OF_3(BDC)_3)$]·nH_2O)	1598	5, 9	25, 29	320	Several analytes	Packed column	[119]	2013
	1652 alone, 565 with		5.72, 17.9		Endocrine disrupting	Core–shell		
ZIF-8, Zn(2-methylimidazole)$_2$	SiO_2	Pore volume of 0.48 $cm^3\,g^{-1}$		280	chemicals and pesticides	microspheres packed column ZIF-8@SiO_2	[120]	2013
Other chromatographic methods								
MOF-5, IRMOF-1 ($Zn_4O(BDC)_3$)		7.5, 11.2	11, 15	400–480	Organic dyes	Single crystal	[121]	2010
ZIF-8, Zn(2-methylimidazole)$_2$	1947	3.4	11.6	≈450	Phenolic isomers	PSP[c] for C-EKC[d]	[122]	2012
MIL-100(Fe), ([$(Fe_3OF_3(BDC)_3)$]·nH_2O)		5, 9	25, 29		Small organic molecules	Coated capillary for CEC[e]	[124]	2013
CAU-1, ([$Al_8(OH)_4$-$(OCH_3)_8$(BDC-$NH_2)_6$])	1700 alone, 423 with polymer		4.5, 10		Aromatic carboxylic acids & some model drugs	Composite with P-MA[f] coated capillary for CEC	[126]	2013
MIL-101(Cr), ($Cr_3O(H_2O)_2F(BDC)_3$)	2938 alone, 732 with polymer				Various aromatics	Composite with PMA monolithic capillary for CEC & nano-LC	[127]	2013
UiO-66, [$Zr_6O_4(OH)_4(BDC)_6$]	881 alone, 321 with polymer				Various aromatics	Composite with PMA monolithic column for HPLC	[128]	2013

Table 1 (*Continued*)

MOF material	Surface area ($g\,cm^{-3}$)	Pore opening (Å)	Pore diameter (Å)	Thermal stability (°C)	Samples	Form	Ref.	Year
$Co(D\text{-}Cam)_{1/2}(BDC)_{1/2}(tmdpy)$				250	Racemates	Chiral GC separation	[131]	2013
$Zn(ISN)_2{\cdot}2H_2O$				350	Racemates	Chiral GC separation	[134]	2013
$Ni(D\text{-}Cam)(H_2O)_2$				250	Racemates	Chiral GC separation	[132]	2014
$[Cu_2(D\text{-}Cam)_2(4,4'\text{-}bpy)]_n$		19.4, 22.4	5		Racemates	Chiral HPLC separation	[133]	2014

[a] Persistent organic pollutants.
[b] Volatile organic compounds.
[c] Pseudostationary phase.
[d] Capillary electrokinetic chromatography.
[e] Capillary electrochromatography.
[f] Poly-methacrylate.

of entropy during adsorption compared to n-hexane. The cyclic molecule loses less freedom in the interwoven structure of small (~8 Å) and large (11 Å) pores in UiO-66 compared to the linear n-hexane molecule.

The physicochemical properties of MOF-5 were determined using inverse gas chromatography (IGC) by Luebbers et al. [83]. They utilised micropacked capillary columns to investigate the effect of structural degradation upon volatile organic compounds (VOCs) adsorption using more than 30 VOCs on MOF-5. MOF-5, which has a surface area of ≈1000 $m^2\,g^{-1}$, is characterised by cages that are approximately 15 Å across and connected by pore openings of approximately 7.5 Å. The results indicated that the samples of MOF-5 experienced a moderate amount of structural degradation showed a stronger interaction with adsorbed species than MOF-5 with fewer defects, resulting in higher heats of adsorption. These results show that the mechanisms of interaction of VOCs with MOFs is more complicated and further work is needed to make that process more clear.

Another IGC study was performed to determine the adsorption behaviours of VOCs on three isoreticular metal-organic frameworks (IRMOFs) [84]. For this purpose, Gutiérrez et al. selected three samples of IRMOFs as adsorbents (IRMOF-1, IRMOF-8 and IRMOF-10) and different types of volatile organic compounds (VOCs) as adsorbates. It was found that the adsorption capacity at infinite dilution and the enthalpy of adsorption increased with the cavity diameter of the structures. As a general trend, it was observed that the strength of the interaction increases in the order IRMOF-1 < IRMOF-8 < IRMOF-10 because of the presence of lattice defects, such as metal clusters in the pores, lattice interpenetration, or the increase in the number of carbon atoms of the organic linkers. It was also observed that the specificity of the interactions is related to the chemistry of the organic linkers more than the structure of the IRMOFs because the presence of π-electron rich zones (aromatic rings or double bonds) enhanced the specificity of the interaction by the favoured interaction with the aromatic rings of the organic linker molecules.

3.1.2. Open-tube capillary columns

The first MOF-coated open-tube capillary column for GC separation was reported in 2010 by Gu and Yan [85]. MIL-101[$Cr_3O(H_2O)_2F(BDC)_3$] was used as the stationary phase, and xylene isomers and ethylbenzene (EB) were used as the targets for separation. MIL-101 was chosen as the stationary phase because of its large surface area of 5900 $m^2\,g^{-1}$, unusually large pores (29 and 34 Å), and excellent chemical and thermal stability [86]. The fabricated capillary column was (15 m long × 0.53 mm i.d.), and the MIL-101 films coated on the inner walls of the capillary column had a thickness of approximately 0.4 mm. Only 1 mg of MIL-101 was needed for the fabrication of a capillary column, which is one advantage for capillary columns over packed columns. The MIL-101-coated capillary column showed efficient baseline separation of xylene isomers and ethylbenzene within 1.6 min and with 3800 plates m^{-1} for *p*-xylene (Fig. 4). The excellent and efficient separation using MIL-101-coated capillary columns was due to host–guest interactions, accessible open metal sites (coordinatively unsaturated sites CUSs) and suitable polarity of MIL-101.

ZIF-8 [Zn(2-methylimidazole)$_2$] has been explored by Chang et al. as a molecular sieving material [87]. The molecular sieving effect is known as the preferential adsorption of molecules with smaller kinetic diameters than the bulkier ones in the micropores [88]. The large pores (11.4 Å) of ZIF-8 along with the 3.4 Å pore openings were found to have the ability to separate linear alkanes from branched alkanes in coated capillary columns. The molecular sieving effect of ZIF-8 led to the separation of branched alkanes from linear alkanes; however, the branched isomers were not completely separated from each other (Fig. 5). The same

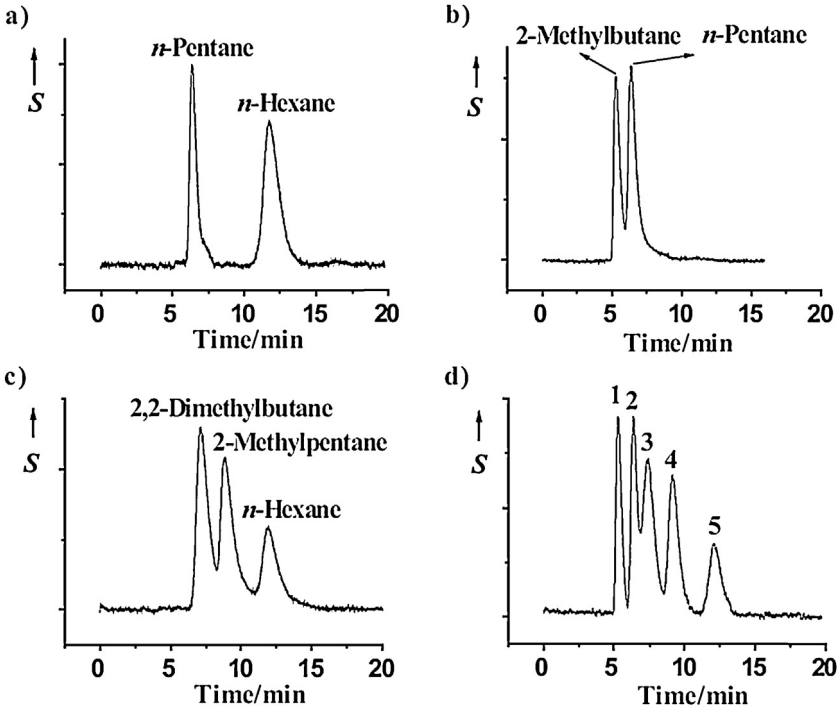

Fig. 2. Chromatograms of alkane mixtures separated on a MOF-508 column: (a) separation of n-pentane and n-hexane, (b) separation of 2-methylbutane and n-pentane, (c) separation of 2,2-dimethylbutane, 2-methylpentane, and n-hexane, and (d) separation of an alkane mixture containing 2-methylbutane (1), n-pentane (2), 2,2-dimethylbutane (3), 2-methylpentane (4), and n-hexane (5). S = thermal conductivity detector response.
Reprinted from Ref. [74]. Copyright 2006 Wiley-VCH.

research group produced an elegant combination of ZIF-8-coated fibres for solid phase micro-extraction (SPME) using a ZIF-8-coated capillary for subsequent GC separation [89]. They demonstrated a MOF-based tandem molecular sieve platform for the selective microextraction of n-alkanes and high-resolution GC separation in complex petroleum-based fuels and human serum samples. A combination of a ZIF-7 [Zn(benzimidazolate)$_2$]-coated SPME fibre with a MIL-101 [$Cr_3O(H_2O)_2F(BDC)_3$]-coated capillary GC has also been examined, revealing the ability to selectively extract benzene homologues and the high-resolution separation of substituted benzene derivatives [89]. This dual-platform combination provides new possibilities for real sample analysis because of the large diversity of MOF structures.

Another molecular sieving material has been tested for coated capillary columns in GC separations. Chang and Yan estimated the reverse-shape selectivity of the molecular sieving MOF material UIO-66 with BDC as the organic linker [88]. UIO-66 has cubic, rigid, 3D-pore structure consisting of octahedral cavities with diameters of 11 Å and tetrahedral cavities with diameters of 8 Å. The accessibility of the cavities is ensured by the microporous triangular windows with diameters in the range of 5–7 Å, which is close to the critical diameter of alkanes and benzene homologues. It

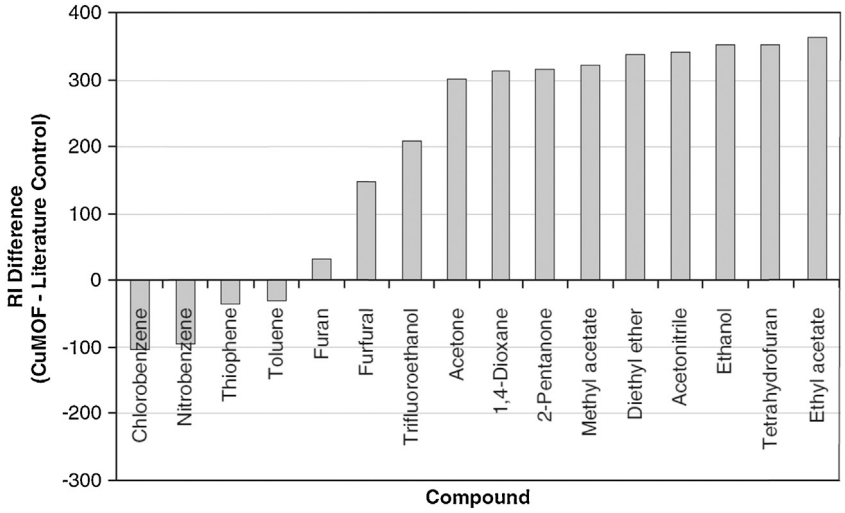

Fig. 3. Graphic showing the retention selectivity of Lewis-base analytes and other probes. The ordinate values are the retention index (RI) differences between the Kováts indices determined on the 0.75% Cu-BTC experimental column minus the SE-30 control Kováts indices extracted from the literature. Positive values indicate that Cu-BTC provided selectivity for the *n*-alkanes. Negative values indicate that SE-30 provides more selectivity than the Cu-BTC. The limitations are discussed in the text.
Reprinted from Ref. [78]. Copyright 2011 Wiley-VCH.

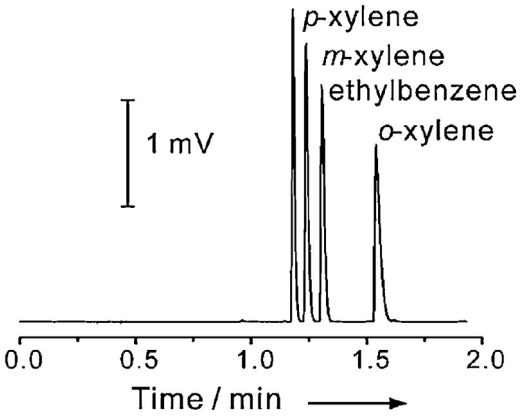

Fig. 4. GC separation of xylene isomers and EB on a MIL-101-coated capillary column at 160 °C with an N_2 flow rate of 3 ml/min.
Reprinted from Ref. [85]. Copyright 2010 Wiley-VCH.

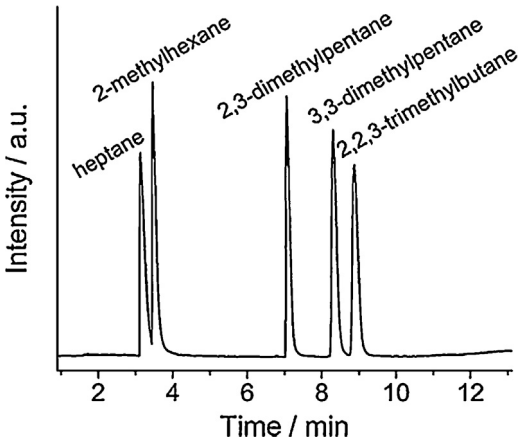

Fig. 6. Gas chromatograms of alkane isomers obtained using an UIO-66-coated capillary column (20 m long × 0.25 mm i.d.) using a temperature program (100 °C for 1 min, then 10 °C min^{-1} to 200 °C).
Reprinted from Ref. [88]. Copyright 2012 Elsevier.

was found that a UiO-66-coated capillary column affords stronger retention for branched alkanes than their linear isomers (Fig. 6). The reverse-shape selectivity of UIO-66 was related to the stronger van der Waals interactions between the side methyl groups on the alkane chains and the pore walls. Additionally, the differences in the polarisabilities of the C—H groups of the branched alkanes could vary the direct dipole-induced hydrogen bonding between the acid sites of UiO-66 and the alkanes, resulting in reverse-shape selectivity [90]. However, the bulkier 1,3,5-trimethylbenzene appeared to elute earlier than the less bulky n-propylbenzene and isopropylbenzene. This result is due to the narrow pore window of UIO-66, which prevents the bulkier 1,3,5-trimethylbenzene from passing into the micropores.

The effect of the metal ion in isostructural MOFs on the chromatographic separation has been investigated by Fan and Yan [91]. The isostructural metal-organic frameworks MIL-100(Fe) [$(Fe_3OF_3(BDC)_3)\cdot nH_2O$] and MIL-100(Cr) [$(Cr_3OF_3(BDC)_3)\cdot nH_2O$], which have identical organic linkers but different metal ions, were used as the stationary phases in the capillary gas chromatographic separation of alkane isomers. The MIL-100(Fe)-coated columns offered excellent features for capillary gas chromatographic separation of alkane isomers with excellent reproducibility, even better than commercial capillary columns, whereas the MIL-100(Cr)-coated capillary column produced poor separation (Fig. 7). The McReynolds constants were used to describe the polarities of the MIL-100 columns. The larger McReynolds constants of the MIL-100(Cr)-coated column indicate that MIL-100(Cr) shows a stronger hydrogen bonding ability than MIL-100(Fe). Moreover, According to the molecular simulation studies by Nicholson and Bhatia [92], Fe(III) has a smaller radius and stronger electrostatic Coulomb interaction with the oxygen in the framework than Cr(III). Therefore, MIL-100(Fe) donates less partial negative charge to the framework oxygen, which in turn weakens the C—H···O bonds between the CH groups of the alkanes and the framework oxygen atoms compared with MIL-100(Cr).

The dynamic coating method [93,94] is the primary method for preparing capillary columns coated with MOFs for GC separations. This procedure is performed by slowly flushing slurries of these materials through fused silica capillaries. The MOF-coated capillaries, using dynamic coating technique, come closest to the ideal porous layer open tubular (PLOT) columns, although they possess significantly larger pore sizes than MOFs. However, the major disadvantage of these coatings is the column bleeding due to spiking, which is the detachment of small particles from the coatings over time that appears as spikes in the chromatograms if a particle filter is not used [95]. Crosslinking of the stationary phase material and chemical bonding of the coatings to the column overcome the bleeding problem. Columns of this type are commercially labelled as “bonded PLOT columns” [96]. Likewise, another technique reported by Münch et al. to prepare MOF-coated capillaries is the cyclic deposition method based on the so-called “controlled SBU-approach” (CSA) for MOF-5 [95] and MOF-199 [97]. This technique forms a thin MOF layer through bonding of the MOF to the substrate surface via a self-assembled monolayer (SAM). The preparation of a SAM provides a layer that serves as an adhesive primer

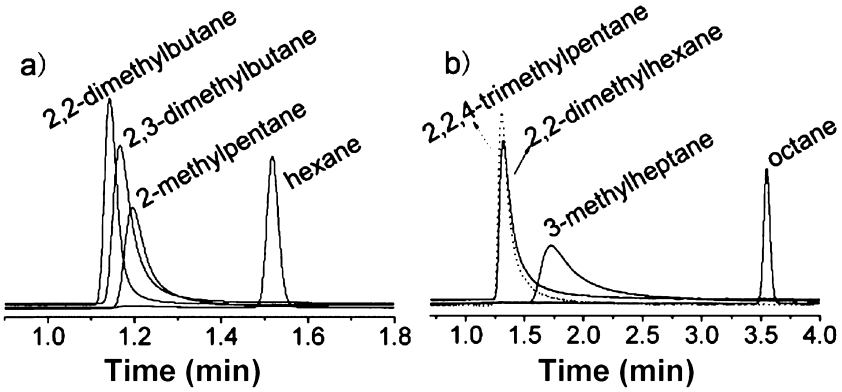

Fig. 5. Chromatograms on ZIF-8-coated capillary (20 m long × 0.25 mm i.d.) for GC separation: (a) hexane and its branched isomers and (b) octane and its branched isomers.
Reprinted from Ref. [87]. Copyright 2010 American Chemical Society.

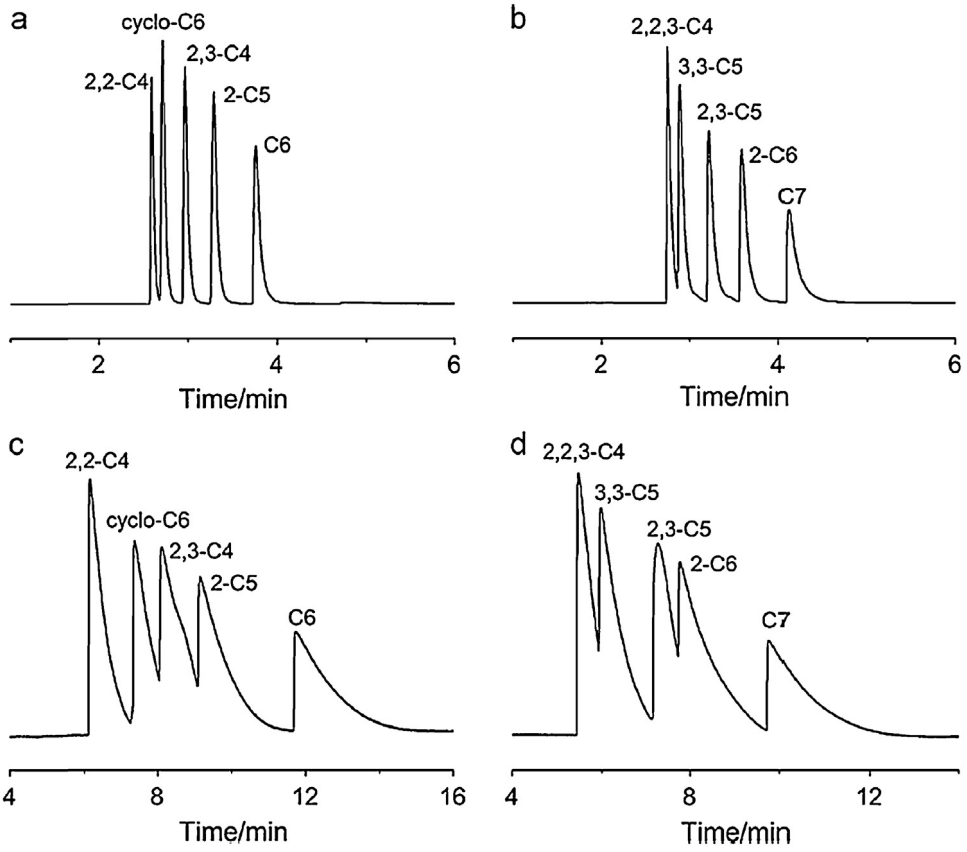

Fig. 7. Chromatograms on MIL-100(Fe) (6 mg ml^{-1}) (a and b) and MIL-100(Cr) (6 mg ml^{-1}) (c and d) coated capillary columns (20 m long × 0.25 mm i.d.): (a and c) C6 group: 2,2-C4 (2,2-dimethybutane), cyclo-C6 (cyclohexane), 2,3-C4 (2,3-dimethybutane), 2-C5 (2-methypentane), and C6 (hexane) with an N_2 flow rate of 1.0 ml/min at 80 °C and (b and d) C7 group: 2,2,3-C4 (2,2,3-trimethybutane), 3,3-C5 (3,3-dimethypentane), 2,3-C5 (2,3-dimethypentane), 2-C6 (2-methyhexane) and C7 (heptane) with an N_2 flow rate of 1.0 ml/min at 110 °C.

Reprinted from Ref. [91]. Copyright 2012 Elsevier.

and allows for the growth of the MOF components (after a layer of SBUs) on the fused silica of standard chromatographic capillaries [95]. The exchange reaction between the monotopic ligands of the SBU precursor and the multitopic linkers leads to interconnection of the SBUs to form the 3D network structure [98].

The MOF-CSA column is mainly used for the analysis of permanent gases and low-molecular-weight hydrocarbons. MOF-5-CSA and MOF-199-CSA columns were used for natural gas separations [95,97]. The performance of the MOF-5-CSA column was equivalent, if not superior, to the leading technology for analytical natural gas separation (Fig. 8); it displayed great stability over five months, performing more than 300 chromatographic separations (in the range 40–150 °C) without any significant loss of separation power [95]. Conversely, the MOF-199-CSA column presented a less suitable separation of natural gas than a similar MOF-5-CSA column [97]. Böhle and Mertens also use the same technique to prepare DMOF-1 [$Cu_2(BDC)_2(DABCO)$] (DABCO; 1,4-diazabicyclo(2,2,2)octane)-coated capillary for the GC separation of light hydrocarbons [99]. They used a layer-by-layer deposition technique developed by Fischer et al. [100] and Wöll et al. [101] to enable the preparation of non-interpenetrating large pore DMOF-1-type frameworks on various surfaces. The fabricated column (10 m long × 0.53 mm i.d.) exhibits high separation power for the light hydrocarbons C_1—C_7. The cyclic CSA method for the preparation of MOF-coated capillaries may add new features, such as controlled growth on the molecular scale or the possibility of creating heterostructures [97].

MOF-CJ3 [$(HZn_3(OH)(BTC)_2(2H_2O)$ (DMF))·H_2O] [102] was selected as a gas chromatography stationary phase by Fang et al.

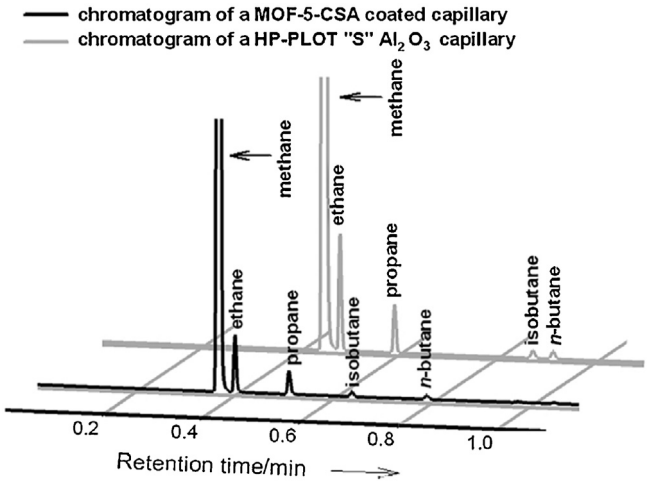

Fig. 8. Comparison of two chromatograms of natural gas (Freiberg, Germany, April 2010) obtained using the MOF-5-CSA-coated column (black line) and an Al_2O_3-based, Na_2SO_4-deactivated commercial PLOT column (Agilent HP-PLOT "S") (grey). MOF-5-CSA-coated column: (10 m long × 0.53 mm i.d.) with 1-mm coating thickness. Carrier gas: He; flow rate: 9.96 ml/min; oven: 80 °C for 0.01 min and 80–140 °C at 60 °C min^{-1} for 1 min; injector: split: 5.1:1 at 250 °C; detector: FID at 250 °C; HP-PLOT "S": (15 m long × 0.53 mm i.d.) with 15-mm coating thickness; carrier gas: He; flow: 9.93 ml/min; oven: 90 °C for 0.01 min and 90–130 °C at 40 °C min^{-1} for 1 min; injector: split: 5.1:1 at 250 °C; detector: FID at 250 °C.

Reprinted from Ref. [95]. Copyright 2011 Wiley-VCH.

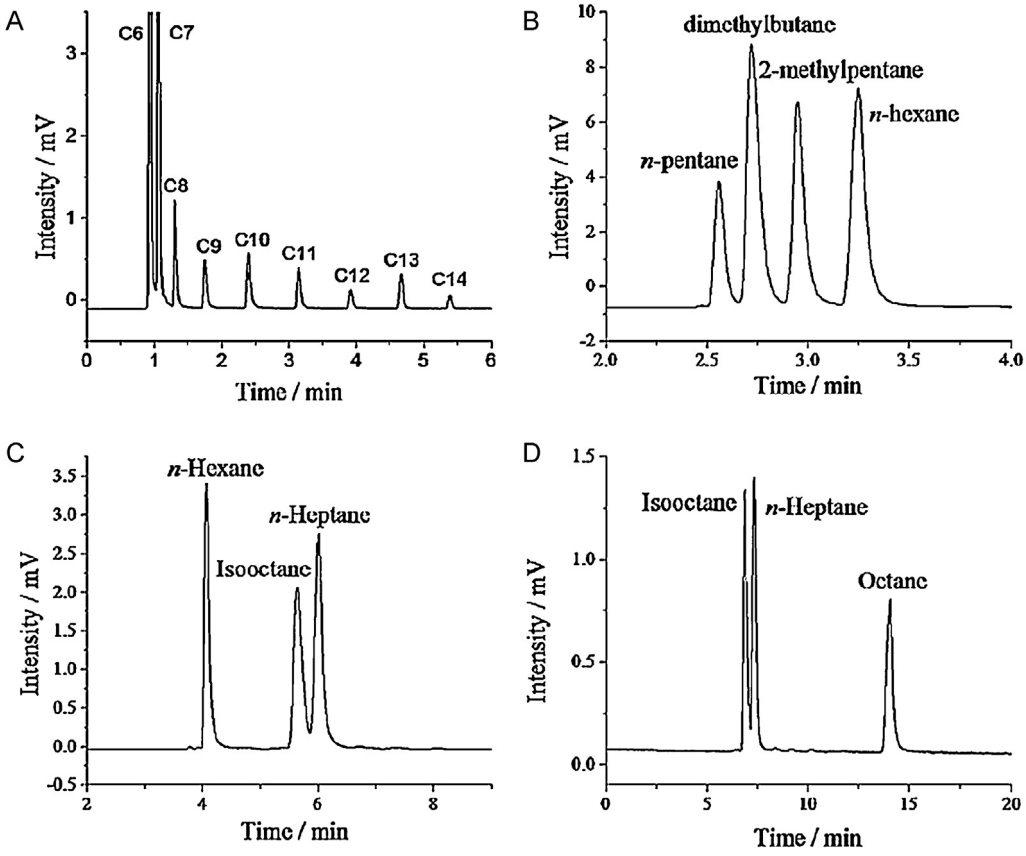

Fig. 9. Gas chromatograms on an MOF-CJ3-coated capillary (10 m long × 0.32 mm i.d.) for separation of alkanes with FID for detection: (A) linear alkanes with an N_2 flow using a temperature program of 80 °C for 1 min, then 20 °C min^{-1} to 180 °C; (B) n-pentane, dimethylbutane, 2-methylpentane and n-hexane with an N_2 flow at 40 °C; (C) n-hexane, isooctane and n-heptane with an N_2 flow at 40 °C; (D) isooctane, n-heptane and octane with an N_2 flow at 40 °C.
Reprinted from Ref. [103]. Copyright 2013 Elsevier.

[103]. MOF-CJ3 possesses extended 1D tubular channels. Its pore wall is composed of BTC ligands, which can provide benzene rings and carboxyl groups to form supramolecular interactions. A relatively short column (10 m long × 0.32 mm i.d.) has been used to separate various types of hydrocarbons, such as linear and branched alkanes, xylene isomers, EB, and aromatic positional isomers (Fig. 9). The theoretical plate numbers obtained from substituted aromatic compounds are in the 361–1466 plates m^{-1} range for this GC column, which is lower than other MOF-based capillary columns. The 1D tubular pores of MOF-CJ3 possess dimensions of 11.6 Å × 11.6 Å, which are accessible to both linear and branched alkanes; therefore, the retention of alkanes on this column depends mainly on the van der Waals forces between the analyte molecules and the MOF materials [103].

3.2. High-performance liquid chromatography applications

Although high-performance liquid chromatography (HPLC) remains the least common chromatographic application for MOFs, it represents an area in which continuing research may reveal many new and superior stationary phases for HPLC. Several MOFs have been studied for HPLC applications [104,112–120]. However, there are many types of MOFs that have not yet been studied for HPLC. The application of MOFs in HPLC, including normal and reverse phase, also requires examining single or binary mobile phases.

MIL-47(V) [$V^{IV}O$(BDC)] and MIL-53(Al) [Al^{III}(OH)(BDC)] were the first MOF materials to be used in LC applications by Alaerts and co-workers [104]. The pore architectures of these materials are similar (one-dimensional pores), and they were fully characterised by Férey and co-workers, who revealed a novel series of MOFs with new topologies [105–111]. MIL-47 has a pore volume of 0.32 cm^3 g^{-1} and a surface area of 750 m^2 g^{-1}, whereas MIL-53 has a pore volume of 0.50 cm^3 g^{-1} and a surface area of 940 m^2 g^{-1} [112]. The main difference between MIL-47 and MIL-53 is the presence of OH vertices in MIL-53, resulting in a highly flexible character, while MIL-47 does not contain OH groups, which makes it more rigid [112].

First, the competitive adsorption equilibria of liquid mixtures of EB and xylene isomers in hexane were studied. MIL-47 preferred *p*-xylene over *m*-xylene with a selectivity of 2.9:1, whereas MIL-53(Al) hardly distinguished between these isomers [104]. In a breakthrough pulse chromatographic experiment, a ternary mixture of EB, *m*-xylene, and *p*-xylene was injected into an MIL-47-packed column in a normal phase system with hexane as the desorbent flowing at 4 ml/min through the column. Three well-separated peaks were obtained in the chromatogram (Fig. 10). The selectivities were 9.7:1 for *p*-xylene vs. EB and 3.1:1 for *p*-xylene vs. *m*-xylene. The isotherms for *p*-xylene and *o*-xylene reached a plateau of 35–37 wt%, which shows that *p*-xylene is packed more easily inside the MIL-47 pores than *m*-xylene or EB [104].

The same research group continued their work on MIL-47 and MIL-53. They performed an interesting comparison on the adsorption of alkylaromatics on both materials [112,113]. On MIL-47, *o*- and *p*-ethyltoluene are almost equally preferred and are more strongly retained than *m*-ethyltoluene (Fig. 11a). Improved separation occurs at higher alkylaromatic concentrations. Conversely, MIL-53(Al) possessed different selectivity patterns; the *o*-isomer elutes later than the other isomers, which are not separated from each other (Fig. 11b) [113]. The different interaction strengths were responsible for this order of selectivity. They

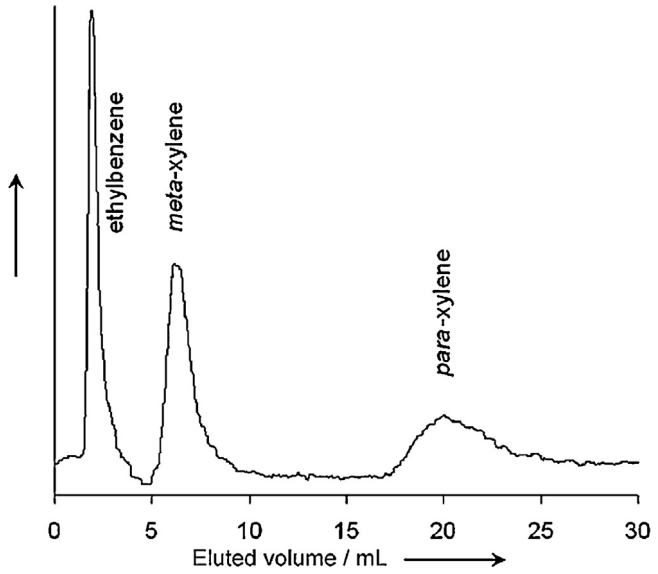

Fig. 10. Chromatographic separation of a mixture of EB, *m*-xylene, and *p*-xylene on a column packed with MIL-47 in the liquid phase and hexane as the desorbent at 298 K. The signal intensity of the refractive index detector is shown versus the eluted volume.
Reprinted from Ref. [104]. Copyright 2007 Wiley-VCH.

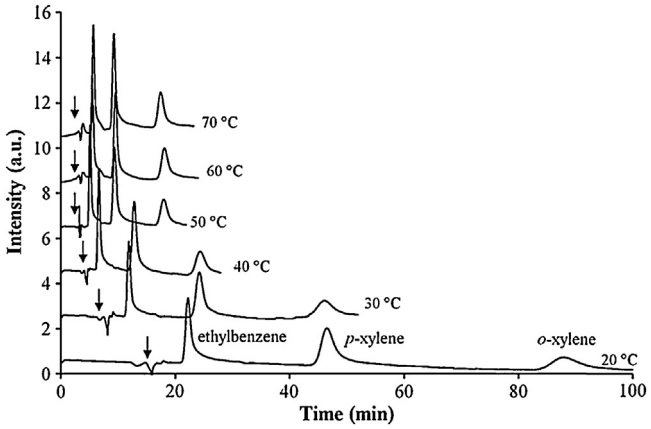

Fig. 12. Influence of the temperature on the retention time of ethylbenzene, *p*-xylene and oxylene (2.25×10^{-4} M, 400 nl), at a flow rate of 1.5 μl min^{-1} (mobile phase 75/25 AN/1-propanol). The chromatograms are gradually shifted by 2 units for clarity. The arrow indicates the injection induced disturbance in the baseline.
Reprinted from Ref. [115]. Copyright 2012 Elsevier.

also suggested that MIL-47 selectively adsorbs the *p*-isomer from *para–meta* mixtures of disubstituted aromatics, such as ethyltoluenes, xylenes, dichlorobenzenes, toluidines and cresols. This preference in adsorption was found to be dependent on the external concentration, which subsequently depends on the functional groups, molecular packing, stearic hindrance and hydrogen bonding [112].

The adsorption selectivities for mono- and di-substituted alkylaromatics with various alkyl groups in MIL-47 and MIL-53 were investigated by determining the adsorption enthalpies at low or high loading using either pulse chromatographic or calorimetric methods [114]. It was found that the separation of cumene (isopropylbenzene) and n-propylbenzene on MIL-47 is an enthalpy-based separation because the uptake of cumene on MIL-47 is enthalpically less favoured than that of n-propylbenzene due to the presence of a branched isopropyl group. Furthermore, as the length of the alkyl chain of n-alkylbenzenes increased, the adsorption enthalpy also increased. While the preferential adsorption of xylenes over EB on MIL-47 was found to be controlled via entropic effects, the preference for xylenes over EB in MIL-53 was due to enthalpic effects [114].

De Malsche et al. reported that the separation of EB, *p*-xylene and *o*-xylene using a glass capillary column (11.6 cm long × 0.15 mm i.d.) packed with MIL-53(Al) showed an unusual pressure drop when the temperature was increased (Fig. 12) [115]. These drops are attributed to the breathing effect of the flexible MIL-53(Al) structure. The degree of expansion of MIL-53(Al) as a function of temperature could be useful for pressure-controlled separations. Moreover, this behaviour could provide a successful method for faster separations at higher temperatures without influencing the selectivity.

Yan and co-workers made a significant development in the liquid chromatographic applications of MIL-47 and MIL-53. They explored the use of a binary mobile phase with a MIL-53(Al)-packed column for HPLC separations. The utilisation of a hexane/dichloromethane or dichloromethane/methanol binary mobile phase provided high-resolution separations of xylene, dichlorobenzene, chlorotoluene, and nitrophenol isomers [116]. The baseline separations were achieved with 10,200 plates m^{-1}

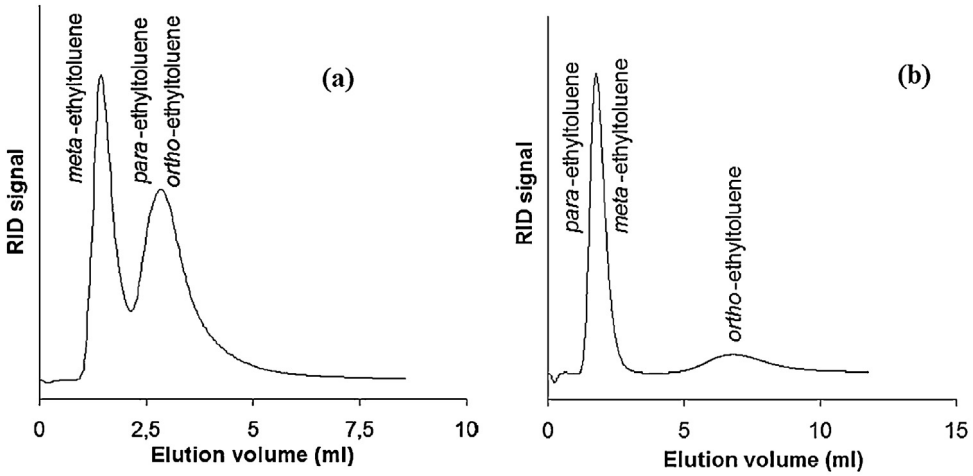

Fig. 11. Chromatographic separation of a mixture of (a) ethyltoluene isomers on a column packed with MIL-47 and (b) ethyltoluene isomers on a column packed with MIL-53 and hexane as the desorbent at 25 °C. The signal intensity of the RID is shown versus the eluted volume. The curves have been corrected for the dead volume of the column.
Reprinted from Ref. [113]. Copyright 2008 American Chemical Society.

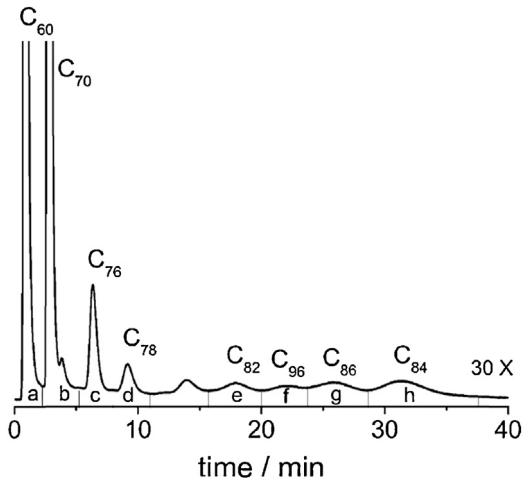

Fig. 13. HPLC separation of the fullerenes in the toluene solution of carbon soot (2.63 mg ml^{-1}) on a MIL-101-packed column (5 cm long × 4.6 mm i.d.) at room temperature with CH_2Cl_2/CH_2CN (98:2) as the mobile phase at a flow rate of 1 ml/min with UV detection at 340 nm.
Reprinted from Ref. [118]. Copyright 2011 Wiley-VCH.

column efficiency for EB and a high resolution. Moreover, the first reverse-phase separation on HPLC (RP-HPLC) using MOF materials was also reported by the same group [117]. High-resolution separations of a wide range of analytes, from non-polar to polar and acidic to basic solutes, were achieved using stainless-steel columns (7 cm long × 4.6 mm i.d.) packed with MIL-53(Al) and CH_3CN/H_2O as the mobile phase. The separations depended on the combined mechanisms of size-exclusion, shape selectivity and hydrophobicity [117].

MIL-101 is another MOF material that has been used for HPLC separations. A MIL-101 packed column (5 cm long × 4.6 mm i.d.) in combination with CH_2Cl_2/CH_2CN (98:2) as the mobile phase has been utilised for the separation of fullerenes [118]. A high-resolution, rapid separation of C_{60} and C_{70} was achieved within 3 min with superior selectivity (R(C70/C60) = 17) and a high column efficiency of 13,000 plates m^{-1} for C_{70}. The MIL-101-packed column was also examined for the separation of the higher fullerenes (C_{76}, C_{78}, C_{82}, C_{84}, C_{86}, and C_{96}) (Fig. 13). It was concluded that the exceptional selectivity of MIL-101 for fullerenes results from several factors, including the difference in the solubility of fullerenes in the mobile phase, diffusion through the pores of MIL-101, and π–π and van der Waals interactions between the fullerenes and the inner walls of the pores of MIL-101 [118].

Recently, MIL-100(Fe) [$(Fe_3OF_3(BDC)_3)$. nH_2O] was explored by Yan's group as a stationary phase for both normal-phase (NP) and reverse-phase (RP) HPLC [119]. In the RP-mode, two groups of neutral and basic analytes were used to test the separation performance of MIL-100(Fe), whereas chloroaniline and toluidine isomers were used for the NP-mode (Fig. 14). Baseline separation of all analytes was obtained with good precision and excellent reproducibility. However, relatively low column efficiency was observed (11,262 plates m^{-1} for *o*-chloroaniline) for the lab-made MIL-100(Fe) packed column due to the irregular particle shapes. The mobile phase composition had a significant effect on both the RP-HPLC and NP-HPLC separations. The thermodynamic study of the MIL-100(Fe) column indicated an exothermic RP-HPLC separation and an endothermic NP-HPLC separation. The selectivity changed significantly with the temperature, indicating the capacity for temperature-dependent separations on MIL-100(Fe)-packed column. The negative ΔG values indicated a spontaneous transfer of all analytes from the mobile phase to the stationary phase. The MIL-100(Fe) MOF material was found to be a successful candidate for both RP and NP-HPLC separations based on the π–π, hydrogen bond and coordination interactions, which resulted from the presence of the aromatic rings, the carboxyl groups and the metal active sites [119].

The irregular shape of MOFs and the size variations lead to lower column efficiency of such MOF-packed columns for HPLC applications. The fabrication of monodisperse MOF@SiO_2 core–shell microspheres as the stationary phase for HPLC was proposed to solve this problem [120]. 400 nm ZIF-8 shell was grown on a carboxyl modified 3.0 μm silica spheres support after three cycles of ZIF-8 growth. No significant increase of ZIF-8 density was noticed with increasing number of growth cycles. The fabricated ZIF-8@SiO_2 core–shell possess a BET surface area of 565.3 m^2 g^{-1}, and a total pore volume of 0.48 cm^3 g^{-1}. A packed columns (5 cm long × 4.6 mm i.d.) with the monodisperse ZIF-8@SiO_2 show a very low column backpressure of 10 bar, and a high efficiency within 7 min for the HPLC separation of endocrine disrupting chemicals (EDCs) and pesticides (23,000 plates m^{-1} for bisphenol A). The high ratio of water (10%, v/v) within the mobile phase significantly decreased the resolution of the EDCs or pesticides separation. The ZIF-8@SiO_2 monodisperse microspheres overcomes the main disadvantage that limits the usage of MOFs as stationary phase for HPLC separation and open up a new field for MOFs application in liquid chromatography [120].

3.3. Other chromatographic applications

In a proof-of-concept experiment, Han et al. demonstrated that chromatographic separations could be performed in a single MOF crystal [121]. They used single MOF-5 crystals with millimetre-sizes (from approximately 1 mm × 1 mm × 1 mm to 3 mm × 3 mm × 2 mm) as the chromatographic column. The separation of organic dye mixtures was detected using fluorescence confocal microscopy over a distance of only a few hundred micrometres. Dimethylformamide (DMF) was used as the mobile phase because it has no effect on the integrity of the MOF-5 crystal, while other solvents, such as H_2O, CH_3CN, MeOH, CH_2Cl_2, and THF, resulted in crystal cracking. Moreover, the MOF crystal can be reused after simply soaking in fresh DMF for 24 h. A future study on single MOF crystal chromatographic separations will be a great accomplishment in the enormous challenge of miniaturisation in chromatography.

Li et al. utilised MOFs for capillary electrokinetic chromatography (EKC) for the first time [122]. EKC is a relatively new chromatographic technique based on a combination of the high efficiency of capillary electrophoresis (CE) and the selectivity of HPLC [123]. They found that ZIF-8 met the requirements for the pseudostationary phase (PSP) in EKC. A baseline separation of six phenolic isomers within only 4 min was observed with more than 85,000 plates m^{-1} (except for *p*-benzenediol). The unique 3D porous frameworks with a large surface area found in ZIF-8 led to strong interactions between the phenolic hydroxyl groups of the solutes and ZIF-8, which yielded good separation.

Capillary electrochromatography (CEC) is one of the most recent chromatographic techniques to use MOF materials as stationary phases. Xu et al. reported an in situ, self-assembly, layer-by-layer method for fabricating MIL-100(Fe)-coated open-tubular capillary columns for CEC [124]. They proposed a new technique to control the capillary coating with MOF materials. GLYMO-IDA-silane was synthesised through the reaction between 3-glycidoxypropyltrimethoxysilane (GLYMO) and iminodiacetic acid (IDA) according to Zou et al. [125] and attached to the inner walls of the capillaries after etching and chemical modification. $FeCl_3 \cdot 6H_2O$ was then pumped into the capillary, followed by a BTC ethanol solution, to form the first cycle of MIL-100(Fe). Repeating the last step led to a series of open-tubular capillary columns

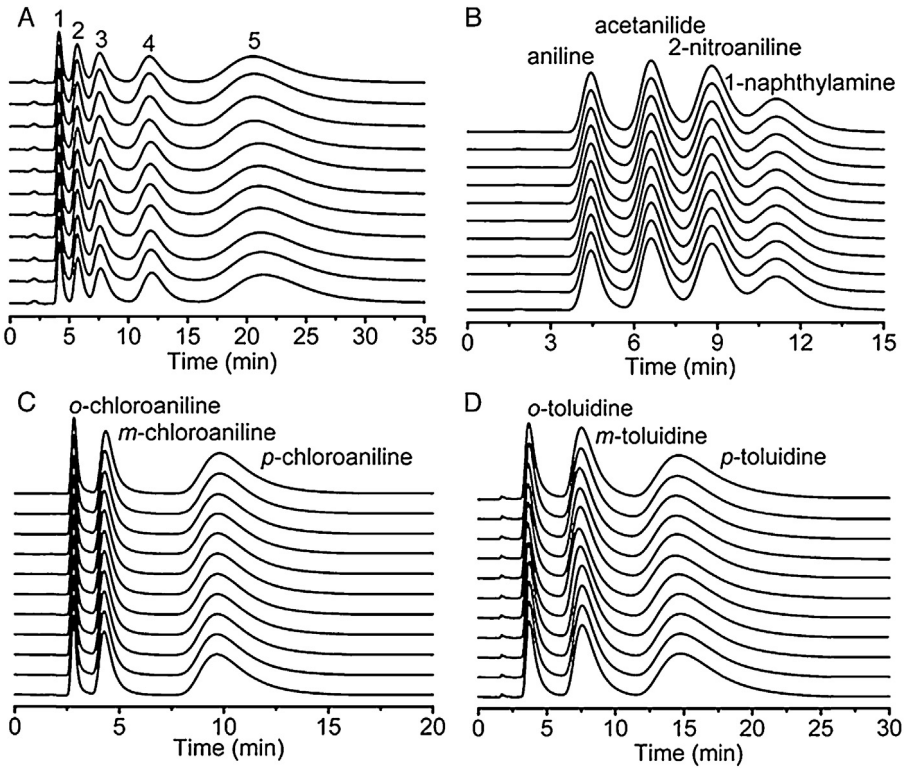

Fig. 14. Reproducibility of the chromatograms for HPLC on a MIL-100(Fe)-packed column (5 cm long × 4.6 mm i.d.): (A) benzene, toluene, ethylbenzene, naphthalene and 1-chloronaphthalene (5 μl, 0.01 mol l^{-1}) using MeOH/H_2O (43:57) as the mobile phase; (B) aniline, acetanilide, 2-nitroaniline and 1-naphthylamine (5 μl, 0.01 mol l^{-1}) using MeOH/H_2O (43:57) as the mobile phase; (C) *o*-, *m*-, and *p*-chloroaniline (5 μl, 0.012 mol l^{-1}) using DCM/MeOH (99.7:0.3) as the mobile phase; (D) *o*-, *m*-, and *p*-toluidine (5 μl, 0.012 mol l^{-1}) using DCM/MeOH (99.7:0.3) as the mobile phase at a flow rate of 0.5 ml/min. All separations were performed at room temperature and monitored using a UV detector at 254 nm.

Reprinted from Ref. [119]. Copyright 2013 Elsevier.

with varying layers of MIL-100(Fe). Neutral, acidic and basic analytes were successfully separated with very good selectivity and excellent reproducibility using a 10-cycle MIL-100(Fe) column. The suitability of MIL-100(Fe)-coated open-tubular capillary columns for different types of analytes was due to the hydrophobicity of the organic ligands and the size selectivity of the lattice aperture. Moreover, the absorbance and quantity of MIL-100(Fe) were found to be proportional to the number of coating cycles.

Metal-organic framework materials in composite polymers are another interesting application in CEC. The incorporation of MOF CAU-1 [$(Al_8(OH)_4$-$(OCH_3)_8(BDC\text{-}NH_2)_6)$] into polymethyl methacrylate (PMMA) to produce CAU-1@PMMA composite was reported for coated open-tubular CEC applications [126]. The solution of CAU-1 and the polymerisation mixture in DMSO was simply passed through a capillary (30 cm long × 0.075 mm i.d.), leaving a thin layer of the solution on the inner wall, which was subsequently thermally polymerised to produce a very rough inner surface. No baseline separations of the selected aromatic acids and nonsteroidal anti-inflammatory drugs were observed on a MOF-free column. However, the composite-coated capillary (CAU-1@PMMA column) achieved a higher efficiency (16,964 plates m^{-1} for ketoprofen and 66,327 plates m^{-1} for benzoic acid), shorter separation time, increased loading capacity for the separation of aromatic acidic compounds and improved resolution of the tested drugs.

Open-tubular capillary columns are not the exclusive form of MOF stationary phases for CEC. MIL-101(Cr) incorporated into a methacrylate polymer (PMA) monolith was developed for CEC and nano-liquid chromatography (nano-LC) [127]. A neat polymer column and a MIL-101(Cr)-packed column were prepared using the same conditions for comparison. Microwave-assisted polymerisation was used to prepare the columns in only 5 min. Efficient separations were achieved for a group of various aromatic compounds (Fig. 15), polycyclic aromatic hydrocarbons (PAHs) and trypsin-digested BSA peptides using a MIL-101(Cr)@PMA monolithic capillary column. The incorporation of the MIL-101(Cr) MOF provided a much larger surface area than the neat polymer and also provided the stationary phase with meso- and nanopores In addition, this hybrid MOF–polymer column possessed high permeability compared to the MOF-packed column, with an approximately 800-fold increase.

UiO-66 incorporated PMA monoliths were successfully used to enhance the HPLC separation of small molecules with high column efficiency and good reproducibility [128]. A stainless-steel column (7 cm long × 4.6 mm i.d.) filled with UIO-66@PMA monolith composite with an average particle size of 210 nm of UIO-66 was utilised to enhance HPLC separation of neutral polycyclic aromatic hydrocarbons, basic aniline series, acid phenol series, and naphthyl substitutes. The prepared column showed an increase in BET surface area (321.4 $m^2\,g^{-1}$) as compared to a similar monolithic column without UIO-66 (192.6 $m^2\,g^{-1}$). Using different concentrations of UiO-66 showed an increase in the retention of the small molecules and their resolutions with the increased amount of the UiO-66 incorporated. The retention and resolution of all of the analytes decreased with increasing the content of ACN in the mobile phase. UIO-66@PMA monolithc column offered a column efficiency of 28,800 plates m^{-1} for 2, 6-dimethylphenol, while monolith without incorporating UiO-66 gave a poor column efficiency (2967–8218 plates m^{-1}). The enhanced separation performance of UiO-66 incorporated PMA monoliths for small molecules mainly resulted from the π–π interaction, the hydrophobic interaction and the interaction between

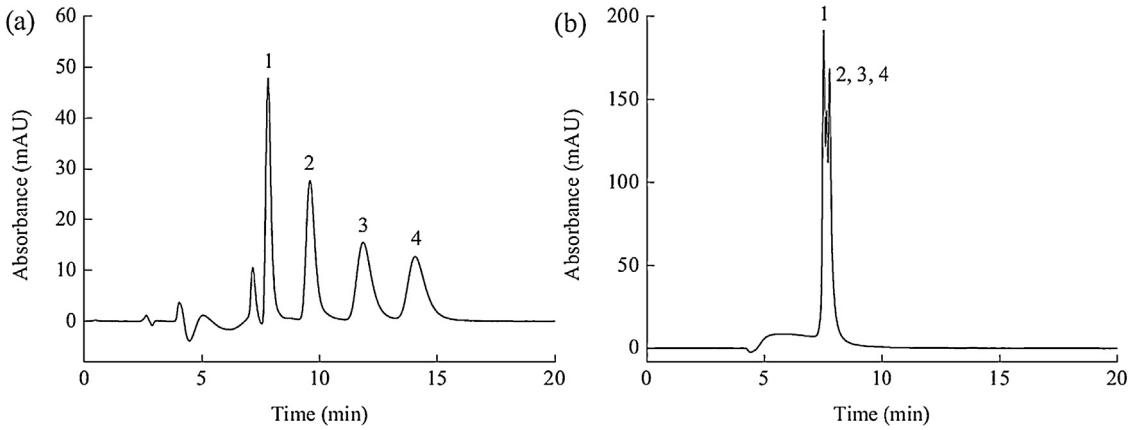

Fig. 15. Nano-UHPLC chromatograms of aromatic acids separated on a MIL-101(Cr)–polymer monolith (a) and a neat polymer monolith (b). The separation conditions were a mobile phase of 0.1% formic acid in water/0.1% formic acid in ACN = 20/80 (v/v), a flow rate of 1 μl min^{-1}, a detection wavelength of 200 nm, an injection volume of 500 nl, an effective length of 35 cm, a column temperature of 25 °C, and an analyte concentration of 10 μg ml^{-1}. 1 (benzoic acid), 2 (terephthalaldehydic acid), 3 (isophthalic acid), 4 (terephthalic acid).

Reprinted from Ref. [127]. Copyright 2013 Elsevier.

the nitrogen atom in the analyte and the Zr active sites in UiO-66 [128].

The separation of racemic mixtures using enantioselective stationary phases is often required. However, it always been a complicated and expensive process. Homochiral metal-organic frameworks (HMOFs) are a new family of MOFs that can serve as Chiral Stationary Phases (CSPs). HMOFs are usually synthesised by using chiral linkers with a metal containing node. Molecular modelling simulations were used by Bao et al. to screen 8 HMOFs for their ability to separate 19 chiral compounds by enantioselective adsorption [129]. They have noticed that there is a lack of correlation between the enantioselectivities of a homologous series of chiral compounds. The shift in the adsorption site was the mean reason for the uncorrelated enantioselectivities, which could be preserved by a smooth HMOF pore [129]. It was demonstrated that there is a strong correlation between the size of the pore and the size of the chiral analyte [130]. Size matching between the chiral HMOF stationary phase and the chiral molecule led to the formation of a tight inclusion complex which increases the enantioselectivity. However, even with size matching exists between the size of the pore and the size of the chiral molecule no enantioselectivities were obtained. Using a slightly different size chiral selector was suggested to solve that problem [130].

Yuan's group employed several D-Cam (D-camphoric acid) based HMOFs as homochiral stationary phases [131–133]. High-resolution gas chromatographic separation was performed on Co(D-Cam)$_{1/2}$(BDC)$_{1/2}$(tmdpy) [tmdpy = 4,4′-trimethylenedipyridine)]-coated open tubular columns [131]. The Co(D-Cam)$_{1/2}$(BDC)$_{1/2}$(tmdpy) structure possesses a 3-D framework with enantiopure building blocks embedded in intrinsically chiral topological nets. They prepared two fused-silica open tubular columns with different inner diameters and lengths, including column A (30 m long × 0.53 mm i.d.) and column B (2 m long × 0.075 mm i.d.), by a dynamic coating method using Co-(D-Cam)$_{1/2}$ (BDC)$_{1/2}$ (tmdpy) as the stationary phase. The number of theoretical plates of the two metal-organic framework columns was 1450 and 3100 plates m^{-1}, respectively, using n-dodecane as the test compound at 120 °C. The LOD (limit of detection) and LOQ (limit of quantification) were found to be 0.125 and 0.417 ng for citronellal enantiomers, respectively. A similar homochiral MOF (Ni(D-Cam)(H_2O)$_2$) was chosen as stationary phase for high-resolution GC separation by the same research group [132]. The experimental results of both stationary phases showed an excellent chiral recognition ability towards racemates due to the chiral microenviroment with its unusual integration of molecular chirality, 3-D intrinsic chiral net, and absolute helicity [131,132].

[Cu$_2$(D-Cam)$_2$(4,4′-bpy)]$_n$ with 3D six-connected self-penetrating architectures was another D-Cam based MOF material used for chiral separation [133]. This study explored some effects such as mobile phase composition, column temperature, and analytes mass for separations using [Cu$_2$(D-Cam)$_2$(4,4′-bpy)]$_n$ homochiral MOF on HPLC. A 4.0 g mass of the prepared material was filled into a stainless steel column (25 cm long × 4.6 mm i.d.) and used for the separations of positional isomers and chiral compounds. A variety of solutes were tested including alcohols, a diol, a naphthol and a ketone racemates. The results proved that [Cu$_2$(D-Cam)$_2$(4,4′-bpy)]$_n$ showed good selectivity for positional isomers and enantiomers. In thermodynamic terms, the negative values of ΔG indicated a spontaneous transfer of analytes from the mobile phase to the stationary phase. The interaction between solutes and the surface of homochiral layers or channels are possibly the main interactive force [133].

A successful chiral separation using Zn(ISN)$_2$·2H_2O [ISN = isonicotinic acid] with a large (~8.6 Å) left-handed channel was performed for high-resolution GC [134]. The column efficiency of Zn(ISN)$_2$·2H_2O-coated column was up to 3020 plates m^{-1}. The separation performance of a dynamic coated capillary column (3 m long × 0.075 mm i.d.) was investigated through a wide range of organic compounds separation. The results showed that Zn(ISN)$_2$·2H_2O stationary phase possesses high column efficiency, good reproducibility, excellent selectivity, and chiral recognition ability.

4. Conclusions

The utilisation of metal-organic frameworks in chromatography has witnessed significant developments over the last five years, with progressive improvements year after year. The unique properties of MOFs provide new properties for chromatographic separations. We have reviewed the most significant and recent advances in MOF applications for HPLC, GC, CEC, and other chromatographic techniques. MOFs have been introduced as packed columns, open-tubular capillary columns, monolithic columns and even as a single crystal column. The packed columns showed excellent performance with significant stability for HPLC and GC. However, the variability in the particle size and irregularity are the greatest challenges. The monodisperse MOF@SiO_2 core–shell microspheres as stationary phase for HPLC has been proposed

recently to overcome the irregularity and size variations problem of MOF packed particles. Another problem accompanied with the packed MOF columns is the high cost due to the need for large amounts of material to fill the packed column. A number of thermodynamic studies using IGC were performed seeking for a deeper under standing of the adsorption nature on MOF materials. However, it needs more researches to get the complete picture.

The open-tubular capillary columns also produce very good results for GC and CEC applications; in addition, they avoid the cost problem of MOF-packed columns. The main disadvantages of open-tubular MOF capillary columns which fabricated via the dynamic coating method is the leak of the material out of the column with time. The SBU-controlled approach has emerged to solve the leakage problem in coated capillaries and to provide a well-controlled method for capillary coating. A successful separation on a single crystal of MOF-5 was performed as a proof-of-concept experiment. This experiment introduces a new horizon of miniaturisation.

Chiral separation is one of the most important and promising MOF application in separation science. Homochiral metal-organic frameworks (HMOFs) are a new revolutionary MOF materials that can serve as Chiral Stationary Phases (CSPs). The enatioselectivity of MOFs emerged from the usage of a chiral linker within the MOF structure giving an infinite probabilities to produce HMOFs for chromatographic separations.

MOF-based hybrid materials such as MOF combination with organic monolithic polymers exhibit a very good performance. A composite column of MOF particles incorporated into a monolithic polymers showed both advantage of high permeability of monolithic materials and the high surface area and high resolution of MOFs for chromatographic separation. Such combinations extend the properties of MOFs to include the advantages of the combined material and even exclude some disadvantages of using MOFs as stationary phase.

The use of MOFs in chromatography has revealed some unexpected behaviours. For example, an unusual pressure drop with increasing temperature was observed for a MIL-53(Al)-packed column in HPLC. Additionally, reverse-shape selectivity was observed with UIO-66 in GC applications.

Although many MOFs have already been examined for chromatographic separations, there are a hundreds of MOF materials that have not been studied for separation science. Furthermore, chromatography has not yet taken advantage of the controllable structure of MOFs to construct new types of MOFs specially designed for specific applications. The precise control of MOF shape, pore size, and chemical nature through the intelligent choice of both the metals and ligands would provide chromatographers unlimited possibilities for stationary phases. Post-synthetic modification of MOFs by adding functional groups may also lead to flexible smart columns that could alter their separation ability according to the analyte. We believe that continued research into the use of MOFs in chromatographic separations will expose many fortuitous and distinctive results.

Acknowledgments

The authors acknowledge the financial support of this work by King Saud University through National Plan for Science and Technology grant # NPST ADV 2120-02.

References

[1] H. Furukawa, K.E. Cordova, M. O'Keeffe, O.M. Yaghi, Science 341 (2013) 974.
[2] H. Gliemann, C. Wöll, Mater. Today 15 (2012) 110.
[3] G. Férey, in: R. Xu, Z. Gao, J. Chen, W. Yan (Eds.), From Zeolites to Porous MOF Materials – The 40th Anniversary of International Zeolite Conference, vol. 170, 2007, p. 66.
[4] E.A. Tomic, J. Appl. Polym. Sci. 9 (1965) 3745.
[5] C. Robl, Mat. Res. Bull. 27 (1992) 99.
[6] B.F. Hoskins, R. Robson, J. Am. Chem. Soc. 112 (1990) 1546.
[7] D. Venketaraman, G.B. Gardner, S. Lee, J.S. Moore, J. Am. Chem. Soc. 117 (1995) 11600.
[8] D. Maspoch, D. Ruiz-Molina, K. Wurst, N. Domingo, M. Cavallini, F. Biscarini, J. Tejada, C. Rovira, J. Veciana, Nat. Mater. 2 (2003) 190.
[9] S.R. Batten, N.R. Champness, X.-M. Chen, J. Garcia-Martinez, S. Kitagawa, L. Öhrström, M. O'Keeffe, M.P. Suh, J. Reedijk, CrystEngComm 14 (2012) 3001.
[10] D.J. Tranchemontagne, J.L. Mendoza-Cortés, M. O'Keeffe, O.M. Yaghi, Chem. Soc. Rev. 38 (2009) 1257.
[11] O.M. Yaghi, H. Li, J. Am. Chem. Soc. 117 (1995) 10401.
[12] O.K. Farha, I. Eryazici, N.C. Jeong, B.G. Hauser, C.E. Wilmer, A.A. Sarjeant, R.Q. Snurr, S.T. Nguyen, A.Ö. Yazaydın, J.T. Hupp, J. Am. Chem. Soc. 134 (2012) 15016.
[13] J. Rocha, M.W. Anderson, Eur. J. Inorg. Chem. 2000 (2000) 801.
[14] C. Serre, F. Taulelle, G. Férey, Chem. Commun. (22) (2003) 2755.
[15] M.I. Khan, L.M. Meyer, R.C. Haushalter, A.L. Schweitzer, J. Zubieta, J.L. Dye, Chem. Mater. 8 (1996) 43.
[16] M. Cavellec, J.M. Grenèche, D. Riou, G. Férey, Chem. Mater. 10 (1998) 2434.
[17] S. Natarajan, S. Neeraj, A. Choudhury, C.N.R. Rao, Inorg. Chem. 39 (2000) 1426.
[18] N. Guillou, Q. Gao, M. Nogues, R.E. Morris, M. Hervieu, G. Férey, A.K.C.R. Cheetham, Acad. Sci. Paris Ser. II 2 (1999) 387.
[19] P. Feng, X. Bu, G. Stucky, Science 278 (1997) 2080.
[20] G. Férey, Chem. Soc. Rev. 37 (2008) 191.
[21] D.-K. Bucar, G.S. Papaefstathiou, T.D. Hamilton, Q.L. Chu, I.G. Georgiev, L.R. MacGillivray, Eur. J. Inorg. Chem. 29 (2007) 4559.
[22] E.R. Parnham, R.E. Morris, Acc. Chem. Res. 40 (2007) 1005.
[23] H. Deng, S. Grunder, K.E. Cordova, C. Valente, H. Furukawa, M. Hmadeh, F. Gándara, A.C. Whalley, Z. Liu, S. Asahina, H. Kazumori, M. O'Keeffe, O. Terasaki, J.F. Stoddart, O.M. Yaghi, Science 336 (2012) 1018.
[24] H. Furukawa, Y.B. Go, N. Ko, Y.K. Park, F.J. Uribe-Romo, J. Kim, M. O'Keeffe, O.M. Yaghi, Inorg. Chem. 50 (2011) 9147.
[25] D.J. Tranchemontagne, Z. Ni, M. O'Keeffe, O.M. Yaghi, Angew. Chem. Int. Ed. 47 (2008) 5136.
[26] G.M. Whitesides, Science 295 (2002) 2418.
[27] O.M. Yaghi, M. O'Keeffe, N.W. Ockwig, H.K. Chae, M. Eddaoudi, J. Kim, Nature 423 (2003) 705.
[28] B. Moulton, M.J. Zaworotko, Chem. Rev. 101 (2001) 1629.
[29] A.J. Blake, N.R. Champness, P. Hubbertstey, W. Li, M.A. Withersby, M. Schroder, Coord. Chem. Rev. 183 (1999) 117.
[30] L. Carlucci, G. Ciani, P. Macchi, D.M. Proserpio, Chem. Commun. 17 (1998) 1837.
[31] L. Carlucci, G. Ciani, D.M. Proserpio, S. Rizzato, J. Chem. Soc., Dalton Trans. (2000) 3821.
[32] L. Carlucci, G. Ciani, D.M. Proserpio, S. Rizzato, Chem. Commun. (2001) 1198.
[33] O.R. Evans, W. Lin, Acc. Chem. Res. 35 (2002) 511.
[34] K. Biradha, Y. Hongo, M. Fujita, Angew. Chem. Int. Ed. 39 (2000) 3843.
[35] O.M. Yaghi, H. Li, T.L. Groy, Inorg. Chem. 36 (1997) 4292.
[36] O.M. Yaghi, H. Li, C. Davis, D. Richardson, T.L. Groy, Acc. Chem. Res. 31 (1998) 474.
[37] M. Eddaoudi, D.B. Moler, H. Li, B. Chen, T.M. Reineke, M. O'Keeffe, O.M. Yaghi, Acc. Chem. Res. 34 (2001) 319.
[38] A. Stein, S.W. Keller, T.E. Mallouk, Science 259 (1993) 1558.
[39] E.J. Corey, Chem. Soc. Rev. 17 (1988) 111.
[40] N.W. Ockwig, O. Delgado-Friedrichs, M. O'Keeffe, O.M. Yaghi, Acc. Chem. Res. 38 (2005) 176.
[41] M. O'Keeffe, M. Eddaoudi, H. Li, T. Reineke, O.M. Yaghi, J. Solid State Chem. 152 (2000) 3.
[42] L. Pauling, J. Am. Chem. Soc. 51 (1929) 1010.
[43] O. Delgado-Friedrichs, M. O'Keeffe, J. Solid State Chem. 178 (2005) 2480.
[44] C. Baerlocher, W.M. Meier, D.H. Olson, Atlas of Zeolite Framework Types, 5th revised ed., Elsevier, Amsterdam, 2001.
[45] M. O'Keeffe, M.A. Peskov, S.J. Ramsden, O.M. Yaghi, Acc. Chem. Res. 41 (2008) 1782.
[46] O. Delgado-Friedrichs, M. O'Keeffe, O.M. Yaghi, Phys. Chem. Chem. Phys. 9 (2007) 1035.
[47] H. Li, M. Eddaoudi, T.L. Groy, O.M. Yaghi, J. Am. Chem. Soc. 120 (1998) 8571.
[48] H. Li, M. Eddaoudi, M. O'Keeffe, O.M. Yaghi, Nature 402 (1999) 276.
[49] H. Furukawa, O.M. Yaghi, J. Am. Chem. Soc. 131 (2009) 8875.
[50] P.J. Fagan, M.D. Ward, Sci. Am. 267 (1992) 48.
[51] M. Eddaoudi, J. Kim, N. Rosi, D. Vodak, J. Wachter, M. O'Keeffe, O.M. Yaghi, Science 295 (2002) 469.
[52] H.K. Chae, D.Y. Siberio-Pérez, J. Kim, Y.B. Go, M. Eddaoudi, A.J. Matzger, M. O'Keeffe, O.M. Yaghi, Nature 427 (2004) 523.
[53] H. Furukawa, N. Ko, Y.B. Go, N. Aratani, S.B. Choi, E. Choi, A.O. Yazaydin, R.Q. Snurr, M. O'Keeffe, Science 329 (2010) 424.
[54] S.S.-Y. Chui, S.M.-F. Lo, J.P.H. Charmant, A.G. Orpen, I.D. Williams, Science 283 (1999) 1148.
[55] X.-S. Wang, S. Ma, D. Sun, S. Parkin, H.-C. Zhou, J. Am. Chem. Soc. 128 (2006) 16474.
[56] D. Sun, S. Ma, Y. Ke, D.J. Collins, H.-C. Zhou, J. Am. Chem. Soc. 128 (2006) 3896.
[57] S. Ma, D. Sun, M. Ambrogio, J.A. Fillinger, S. Parkin, H.-C. Zhou, J. Am. Chem. Soc. 129 (2007) 1858.
[58] X.-S. Wang, S. Ma, D. Yuan, J.W. Yoon, Y.K. Hwang, J.-S. Chang, X. Wang, M.R. Jørgensen, Y.-S. Chen, H.-C. Zhou, Inorg. Chem. 48 (2009) 7519.

[59] J. Lu, A. Mondal, B. Moulton, M.J. Zaworotko, Angew. Chem. Int. Ed. 40 (2001) 2113.
[60] L. Xie, S. Liu, C. Gao, R. Cao, J. Cao, C. Sun, Z. Su, Inorg. Chem. 46 (2007) 7782.
[61] M. Kramer, U. Schwarz, S. Kaskel, J. Mater. Chem. 16 (2006) 2245.
[62] L.J. Murray, M. Dinca, J. Yano, S. Chavan, S. Bordiga, C.M. Brown, J.R. Long, J. Am. Chem. Soc. 132 (2010) 7856.
[63] O. Kozachuk, K. Yusenko, H. Noei, Y. Wang, S. Walleck, T. Glaserc, R.A. Fischer, Chem. Commun. 47 (2011) 8509.
[64] J.L.C. Rowsell, E.C. Spencer, J. Eckert, J.A.K. Howard, O.M. Yaghi, Science 309 (2005) 1350.
[65] O.K. Farha, C.E. Wilmer, I. Eryazici, B.G. Hauser, P.A. Parilla, K. O'Neill, A.A. Sarjeant, S.T. Nguyen, R.Q. Snurr, J.T. Hupp, J. Am. Chem. Soc. 134 (2012) 9860.
[66] S. Brunauer, P.H. Emmett, E. Teller, J. Am. Chem. Soc. 60 (1938) 309.
[67] J. Moellmer, E.B. Celer, R. Luebke, A.J. Cairns, R. Staudt, M. Eddaoudi, M. Thommes, Microporous Mesoporous Mater. 129 (2010) 345.
[68] F. Rouquerol, J. Rouquerol, K. Sing, Adsorption by Powders and Porous Solids Principles, Methodology and Applications Priorities in Research, Academic Press, London, 1999.
[69] A.V. Neimark, K.S.W. Sing, M. Thommes, in: G. Ertl, H. Knoetzinger, F. Schueth, J. Weitkamp (Eds.), Handbook of Heterogeneous Catalysis, vol. 721, second ed., Wiley-VCH Verlag GmbH and Co, KgaA, Weinheim, 2008, p. 721.
[70] K.S. Walton, R. Snurr, J. Am. Chem. Soc. 129 (2007) 8552.
[71] T. Duren, F. Millange, G. Ferey, K.S. Walton, R. Snurr, J. Phys. Chem. C 111 (2007) 15350.
[72] Z.-Y. Gu, C.-X. Yang, N. Chang, X.-P. Yan, Acc. Chem. Res. 45 (2012) 734.
[73] Y. Yu, Y. Ren, W. Shen, H. Deng, Z. Gao, Trends Anal. Chem. 50 (2013) 33.
[74] B.L. Chen, C.D. Liang, J. Yang, D.S. Contreras, Y.L. Clancy, E.B. Lobkovsky, O.M. Yaghi, S. Dai, Angew. Chem. Int. Ed. 45 (2006) 1390.
[75] V. Finsy, H. Verelst, L. Alaerts, D. De Vos, P.A. Jacobs, G.V. Baron, J.F.M. Denayer, J. Am. Chem. Soc. 130 (2008) 7110.
[76] Z.-Y. Gu, D.-Q. Jiang, H.-F. Wang, X.-Y. Cui, X.-P. Yan, J. Phys. Chem. C 114 (2010) 311.
[77] W.O. McReynolds, J. Chromatogr. Sci. 8 (1970) 685.
[78] D. Scott, D. Alison, K.J. Praveen, J. Sep. Sci. 34 (2011) 2418.
[79] T. Borjigin, F.X. Sun, J.L. Zhang, K. Cai, H. Ren, G.S. Zhu, Chem. Commun. 48 (2012) 7613.
[80] M.D. Toni, R. Jonchiere, P. Pullumbi, F.-X. Coudert, A.H. Fuchs, Chem. Phys. Chem. 13 (2012) 3497.
[81] J.H. Cavka, S. Jakobsen, U. Olsbye, N. Guillou, C. Lamberti, S. Bordiga, K.P. Lillerud, J. Am. Chem. Soc. 130 (2008) 13850.
[82] B. Bozbiyik, T. Duerinck, J. Lannoeye, D.E. De Vos, G.V. Baron, J.F.M. Denayer, Microporous Mesoporous Mater. 183 (2014) 143.
[83] M.T. Luebbers, T. Wu, L. Shen, R.I. Masel, Langmuir 26 (2010) 11319.
[84] I. Gutiérrez, E. Díaz, A. Vega, S. Ordónez, J. Chromatogr. A 1274 (2013) 173.
[85] Z.Y. Gu, X.P. Yan, Angew. Chem. Int. Ed. 49 (2010) 1477.
[86] G. Ferey, C. Mellot-Draznieks, C. Serre, F. Millange, J. Dutour, S. Surble, I. Margiolaki, Science 309 (2005) 2040.
[87] N. Chang, Z.-Y. Gu, X.-P. Yan, J. Am. Chem. Soc. 132 (2010) 13645.
[88] N. Chang, X.P. Yan, J. Chromatogr. A 1257 (2012) 116.
[89] N. Chang, Z.-Y. Gu, H.-F. Wang, X.-P. Yan, Anal. Chem. 83 (2011) 7094.
[90] P.S. Barcia, D. Guimaraes, P.A.P. Mendes, J.A.C. Silva, V. Guillerm, H. Chevreau, C. Serre, A.E. Rodrigues, Microporous Mesoporous Mater. 139 (2011) 67.
[91] L. Fan, X.-P. Yan, Talanta 99 (2012) 944.
[92] T.M. Nicholson, S.K. Bhatia, J. Phys. Chem. B 110 (2006) 24834.
[93] J.G. Nikelly, Anal. Chem. 44 (1972) 623.
[94] J.G. Nikelly, Anal. Chem. 44 (1972) 625.
[95] A.S. Münch, J. Seidel, A. Obst, E. Weber, F.O.R.L. Mertens, Chem. Eur. J. 17 (2011) 10958.
[96] C.-X. Yang, S.-S. Liu, H.-F. Wang, S.-W. Wang, X.-P. Yan, Analyst 137 (2011) 133.
[97] A.S. Münch, F.O.R.L. Mertens, J. Mater. Chem. 22 (2012) 10228.
[98] A.S. Münch, M.S. Lohse, S. Hausdorf, G. Schreiber, D. Zacher, R.A. Fischer, F.O. Mertens, Microporous Mesoporous Mater. 159 (2012) 132.
[99] T. Böhle, F. Mertens, Microporous Mesoporous Mater. 183 (2014) 162.
[100] O. Shekhah, H. Wang, M. Paradinas, C. Ocal, B. Schüpbach, A. Terfort, D. Zacher, R.A. Fischer, C. Wöll, Nat. Mater. 8 (2009) 481.
[101] J. Liu, B. Lukose, O. Shekhah, H.K. Arslan, P. Weidler, H. Gliemann, S. Bräse, S. Grosjean, A. Godt, X. Feng, K. Müllen, I.-B. Magdau, T. Heine, C. Wöll, Sci. Rep. 2 (2012) 921.
[102] J.-H. He, Y.-T. Zhang, Q.-H. Pan, J.-H. Yu, H. Ding, R.-R. Xu, Microporous Mesoporous Mater. 90 (2006) 145.
[103] Z.-L. Fanga, S.-R. Zheng, J.-B. Tan, S.-L. Cai, J. Fan, X. Yan, W.-G. Zhang, J. Chromatogr. A 1285 (2013) 132.
[104] L. Alaerts, C.E.A. Kirschhock, M. Maes, M.A. van der Veen, V. Finsy, A. Depla, J.A. Martens, G.V. Baron, P.A. Jacobs, J.F.M. Denayer, D.E. De Vos, Angew. Chem. Int. Ed. 46 (2007) 4293.
[105] T. Loiseau, C. Serre, C. Huguenard, G. Fink, F. Taulelle, M. Henry, T. Bataille, G. Férey, Chem. Eur. J. 10 (2004) 1373.
[106] K. Barthelet, J. Marrot, D. Riou, G. Férey, Angew. Chem. 114 (2002) 291.
[107] G. Férey, C. Mellot-Draznieks, C. Serre, F. Millange, J. Dutour, S. Surblé, I. Margiolaki, Science 309 (2005) 2040.
[108] S. Miller, P. Wright, C. Serre, T. Loiseau, J. Marrot, G. Férey, Chem. Commun. (2005) 3850.
[109] K. Barthelet, J. Marrot, G. Férey, D. Riou, Chem. Commun. (2004) 520.
[110] G. Férey, M. Latroche, C. Serre, F. Millange, T. Loiseau, A. Percheron-Guégan, Chem. Commun. (2003) 2976.
[111] S. Bourrelly, P.L. Llewellyn, C. Serre, F. Millange, T. Loiseau, G. Férey, J. Am. Chem. Soc. 127 (13) (2005) 519.
[112] L. Alaerts, M. Maes, P.A. Jacobs, J.F.M. Denayerb, D.E. De Vos, Phys. Chem. Chem. Phys. 10 (2008) 2979.
[113] L. Alaerts, M. Maes, L. Giebeler, P.A. Jacobs, J.A. Martens, J.F.M. Denayer, C.E.A. Kirschhock, D.E. De Vos, J. Am. Chem. Soc. 130 (2008) 14170.
[114] M. Maes, F. Vermoortele, M. Boulhout, T. Boudewijns, C. Kirschhock, R. Ameloot, I. Beurroies, R. Denoyel, D.E. De Vos, Microporous Mesoporous Mater. 157 (2012) 82.
[115] W. De Malsche, S. Van der Perre, S. Silverans, M. Maes, D.E. De Vos, F. Lynen, J.F.M. Denayer, Microporous Mesoporous Mater. 162 (2012) 1.
[116] C.-X. Yang, S.-S. Liu, H.-F. Wang, S.-W. Wang, X.-P. Yan, Analyst 137 (2012) 133.
[117] S.-S. Liu, C.-X. Yang, S.-W. Wang, X.-P. Yan, Analyst 137 (2012) 816.
[118] C.-X. Yang, Y.-J. Chen, H.-F. Wang, X.-P. Yan, Chem. Eur. J. 17 (2011) 11734.
[119] Y.-Y. Fu, C.-X. Yang, X.-P. Yan, J. Chromatogr. A 1274 (2013) 137.
[120] Y.-Y. Fu, C.-X. Yang, X.-P. Yan, Chem. Eur. J. 19 (2013) 13484.
[121] S. Han, Y. Wei, C. Valente, I. Lagzi, J.J. Gassensmith, A. Coskun, J.F. Stoddart, B.A. Grzybowski, J. Am. Chem. Soc. 132 (2010) 16358.
[122] L.-M. Li, H.-F. Wang, X.-P. Yan, Electrophoresis 33 (2012) 2896.
[123] V.T. Remcho, Chem. Educ. 2 (1997) 1.
[124] Y. Xu, L. Xu, S. Qi, Y. Dong, Z. Rahman, H. Chen, X. Chen, Anal. Chem. 85 (2013) 11369.
[125] S. Feng, C. Pan, X. Jiang, S. Xu, H. Zhou, M. Ye, H. Zou, Proteomics 7 (2007) 351.
[126] L.-M. Li, F. Yang, H.-F. Wang, X.-P. Yan, J. Chromatogr. A 1316 (2013) 97.
[127] H.-Y. Huang, C.-L. Lin, C.-Y. Wu, Y.-J. Cheng, C.-H. Lin, Anal. Chim. Acta 779 (2013) 96.
[128] Y.-Y. Fu, C.-X. Yang, X.-P. Yan, Chem. Commun. 49 (2013) 7162.
[129] B.Y. Bao, L.J. Broadbelt, R.Q. Snurr, Microporous Mesoporous Mater. 157 (2012) 118.
[130] B.Y. Bao, L.J. Broadbelt, R.Q. Snurr, Phys. Chem. Chem. Phys. 12 (2010) 6466.
[131] S.-M. Xie, X.-H. Zhang, Z.-J. Zhang, M. Zhang, J. Jia, L.-M. Yuan, Anal. Bioanal. Chem. 405 (2013) 3407.
[132] S. Xie, B. Wang, X. Zhang, J. Zhang, M. Zhang, L. Yuan, Chirality 26 (2014) 27.
[133] M. Zhang, J.-H. Zhang, Y. Zhang, B.-J. Wang, S.-M. Xie, L.-M. Yuan, J. Chromatogr. A 1325 (2014) 163.
[134] X.-H. Zhang, S.-M. Xie, A.-H. Duan, B.-J. Wang, L.-M. Yuan, Chromatographia 76 (2013) 831.
[135] Z.-Y. Gu, J.-Q. Jiang, X.-P. Yan, Anal. Chem. 83 (2011) 5093.
[136] M.T. Luebbers, T. Wu, L. Shen, R.I. Masel, Langmuir 26 (2010) 15625.
[137] C.-X. Yang, X.-P. Yan, Anal. Chem. 83 (2011) 7144.